Full length Article

The upper palaeozoic Godar–e-Siah Complex of Jandaq: Evidence and significance of a north Palaeotethyan succession in Central Iran

Fabrizio Berra, Andrea Zanchi, Lucia Angiolini, Daniel Vachard, Giovanni Vezzoli, Stefano Zanchetta, Maria Bergomi, Hamid Reza Javadi, Meyssam Kouhpeima

PII: S1367-9120(17)30053-6
DOI: http://dx.doi.org/10.1016/j.jseaes.2017.02.006
Reference: JAES 2959

To appear in: *Journal of Asian Earth Sciences*

Received Date: 26 July 2016
Revised Date: 29 January 2017
Accepted Date: 2 February 2017

Please cite this article as: Berra, F., Zanchi, A., Angiolini, L., Vachard, D., Vezzoli, G., Zanchetta, S., Bergomi, M., Javadi, H.R., Kouhpeima, M., The upper palaeozoic Godar–e-Siah Complex of Jandaq: Evidence and significance of a north Palaeotethyan succession in Central Iran, *Journal of Asian Earth Sciences* (2017), doi: http://dx.doi.org/10.1016/j.jseaes.2017.02.006

THE UPPER PALAEOZOIC GODAR–E-SIAH COMPLEX OF JANDAQ: EVIDENCE AND SIGNIFICANCE OF A NORTH PALAEOTETHYAN SUCCESSION IN CENTRAL IRAN

Fabrizio Berra (1), Andrea Zanchi (2), Lucia Angiolini (1), Daniel Vachard (3), Giovanni Vezzoli (2), Stefano Zanchetta (2), Maria Bergomi (2), Hamid Reza Javadi (4), Meyssam Kouhpeima (4)

1) Dipartimento di Scienze della Terra "A. Desio", Università degli Studi di Milano, Mi, Italy

2) Department of Earth and Environmental Sciences, Milano-Bicocca University, Piazza della Scienza 4, 20126 Mi, Italy

3) 1 rue des Tilleuls, 59152 Gruson, France

4) Geological Survey of Iran, Azadi Square, Meraj Avenue, 13185-1494 Tehran, Iran

Abstract

The Upper Palaeozoic Godar-e-Siah Complex of Jandaq, Central Iran, comprises three isolated, fault-bounded outcrops exposing Palaeozoic fossiliferous carbonates, volcanics and siliciclastics, which are markedly distinct from the surrounding sedimentary successions. The three outcrops, that emerge below Cretaceous and younger sediments, are the Chah Rizab outcrop, the Godar-e-Siah northern outcrop, and the Godar-e-Siah central outcrop. Their sedimentary successions strongly differ from the typical passive margin successions of Gondwanan affinity that characterize the Yazd, Lut and Tabas blocks of Central Iran and the Alborz in North Iran. To understand the origin of these profound differences, we first calibrated the age of the Jandaq successions: U-Pb radiometric zircons ages, obtained from granitoid boulders in the conglomerates at Chah Rizab and in the Godar-e-Siah northern outcrop, gave a Late Devonian to Mississippian age. Biostratigraphic data from brachiopods and fusulinids from the Godar-e-Siah northern and central outcrops indicate a Pennsylvanian age. The age of the successions is thus post-Visean to Pennsylvanian. The

petrographic composition of the siliciclastic deposits indicates the erosion of a magmatic arc. To understand where the Jandaq complex could have been located at that time, we have assessed the palaeobiogeographic affinity of the faunas. The collected brachiopods and fusulinids assemblages are mostly similar to coeval faunas from Spain, Donbass, Urals, and Yukon Territory (Canada) and have a North-Palaeotethyan affinity. The Godar-e-Siah Complex of Jandaq likely represents part of the southern active margin of Eurasia (northern margin of the Palaeotethys), in contrast to the surrounding Central and North Iran blocks, which were at that time located along the southern margin of the Neotethys.

Our investigations confirm a complex palaeogeographic evolution for the studied outcrops, suggesting that they represent fragments of the southern Eurasian active margin - today preserved in NE Iran - displaced by crustal-scale wrench motions related to the opening and closure of the Sabzear Ocean and to the Cenozoic activity of the Great Kavir-Doruneh Fault and its possible precursors.

Keywords: Central Iran; Upper Palaeozoic; North Palaeotethyan succession

1. Introduction

Palaeogeographic reconstructions are nowadays available for most of the Phanerozoic time intervals and for different areas. General scenarios are well-defined thanks to constraints from different datasets (e.g. stratigraphy, palaeomagnetic studies, geochronology, structural geology, palaeobiogeography). Nevertheless, additional data are continuously required to improve our knowledge of timing and areal occurrence of specific events. Palaeogeographic reconstructions are extremely complicate in the case of polyphase orogenic belts, especially when they result from the progressive accretion of different terranes, and were affected by intense post-collisional tectonics. One of this case is the Late Triassic Cimmerian orogenic event, which was preceded by a long-lasting subduction of the Palaeotethys Ocean below the Eurasian margin. The evolution of the complex jigsaw of the Cimmerian terranes, that detached from Gondwana during the Permian and

later accreted to the southern margin of Eurasia, is still under debate. A key area for the understanding of the Cimmerian event is Iran, where remnants of subduction, collisional and post-collisional systems are preserved along the Palaeotethys suture. According to recent publications (Zanchi et al., 2009a and 2009b; Zanchetta et al., 2013; Zanchi et al., 2015; Zanchi et al., 2016), the suture zone approximately runs along the northern side of the present-day Alborz Mountains and their lateral equivalent, from the Talesh Mountains to Mashhad and Fariman in the SE part of the Kopeh Dag.

However, the occurrence of remnants of a late Palaeozoic to Triassic active margin has been recently documented also in Central Iran, otherwise considered part of the northern passive margin of Gondwana for most of the Palaeozoic (Wendt et al., 2002, 2005; Gaetani et al., 2009). These remnants occur south of the Great Kavir-Doruneh Fault, between Jandaq and Anarak (Fig. 1). The Triassic successions of the Nakhlak forearc basin, a few tens of kilometres just north of the town of Anarak (Alavi et al., 2007; Balini et al., 2009; Zanchi et al., 2009b) and the Anarak accretionary prism (Sharkovsky et al., 1984; Bagheri and Stampfli, 2008; Zanchi et al., 2015) document subduction from the late Palaeozoic to the Triassic. Moreover, Bagheri and Stampfli (2008) described upper Palaeozoic successions, possibly related to the Palaeotethys active margin, to the north of this area just south of Jandaq (Fig. 1). This emphasises the importance of carrying out additional geological studies to reconstruct the complex jigsaw puzzle of blocks and terranes that characterizes Central Iran.Despite the preliminary report of Aistov et al. (1984) and the recent advances in the geological knowledge of Jandaq (Bagheri and Stampfli, 2008) , the area was still deserving additional investigations. In particular, the three isolated outcrops (Fig. 2) forming the Godar-e-Siah Complex SW of Jandaq (Aistov et al., 1984) represent key-exposures for the reconstruction of the Palaeozoic evolution of the Palaeotethys realm. The aim of this paper is to present new detailed stratigraphic, structural, petrographic, palaeontological and geochronological investigations performed on these enigmatic successions, and to discuss the obtained results in the frame of the geodynamic evolution of Central Iran during the late Palaeozoic.

2. Geological setting of Central Iran and its evolution

Central Iran forms the internal part of Iran and shows a very complex geological setting. Its most peculiar feature is the occurrence of an upper Mesozoic ophiolitic "ring", which delimits its internal part (Fig. 1). Central Iran is also affected by active strike-slip faults. The E-W trending left-lateral Great Kavir - Doruneh fault, which crosses the northern part of Central Iran, bounds at present the fault system to the north. Active deformation is accommodated within Central Iran by N-S to NNW-SSE trending dextral faults separating the Yazd, Tabas and Lut blocks (Fig. 1). These blocks, which show similar features , comprise a Precambrian metamorphic basement of Gondwanan affinity, intruded by Cadomian intrusives (Ramezani and Tucker, 2003; Rossetti et al., 2015) and locally covered by the Rizu Formation with metavolcanics, quartzites and dolostones followed by the late Ediacaran to lower Cambrian Soltanieh Formation including a thick dolomitic succession. A thick, poorly deformed Cambrian to Triassic succession, similar to the one exposed in the Alborz Mountains, is also discontinuously present in the three different blocks with local differences. This succession records the passive margin history of Central Iran from the Palaeozoic to the early Mesozoic, when it collided with Eurasia causing the formation of the Cimmerian orogen.

An extremely different evolution is instead recorded in the NW corner of Central Iran, where upper Palaeozoic to Triassic units directly related to the evolution of an active margin possibly connected to the Palaleotethys subduction have been recently documented south of the Great Kavir Fault between Anarak and Jandaq. Bagheri and Stampfli (2008) distinguished several units (Fig.1), which mainly include the Anarak Metamorphic Complex (AMC; Zanchi et al., 2009b, 2015; Buchs et al., 2013), the Jandaq Metamorphic Complex (JMC), the Siah-e-Godar Complex and the Nakhlak arc-related succession (Alavi et al., 1997; Balini et al., 2009).

The AMC consists of a poly-metamorphic accretionary wedge characterized by a blue-schist facies metamorphic imprint. It contains several meta-sedimentary units including dismembered ophiolites, which show different tectono-metamorphic evolutions. Recent dating of metamorphic minerals and

crosscutting dikes (Bagheri and Stampfli 2008; Zanchi et al. 2015) constrain the age of metamorphism between about ca. 330 and 290 Ma.

The JMC extends E-W at the latitude of Jandaq just south of the Great Kavir Fault and includes large bodies of amphibolites, staurolite, garnet, mica schists and gneiss intruded by pegmatites. Radiometric ages from the metamorphic amphiboles show both Carboniferous and Jurassic ages, whereas the pegmatites have a Late Triassic age based on an U-Pb single crystal zircon dating (Bagheri and Stampli, 2008). The JMC is juxtaposed to an ophiolitic belt, the Arusan Mélange, of unknown age, which is intruded by Jurassic granitoids (Aistov et al., 1984).

The Siah-e-Godar Complex, which is the subject of this paper, consists of an upper Palaeozoic marine to continental sedimentary succession which escaped metamorphism. Finally, the Nakhlak succession consists of a well-dated arc-related Lower to Middle Triassic marine to continental deposits forming an isolated spur in the desert between the AMC and the JMC (Fig.1; Alavi et al., 1997; Balini et al., 2009). A supra-subduction basement with gabbros and serpentinites occurs in tectonic contact at the base of the arc succession.

The post-Cimmerian evolution is characterized by the deposition, from the end of the Late Triassic to the Early Jurassic of the Nayband and coeval Shemshak units, which unconformably cover the deformed Cimmerian metamorphic rocks and are in turn followed by the latest Jurassic to Lower Cretaceous Chah Palang and the correlative Garedu Red beds formations.

The evolution of Central Iran was also affected by the opening of Mesozoic back-arc basins in response to the main subduction active under the Sanandaj-Sirjan to the west (e.g. Rossetti et al., 2010; Agard et al., 2011), testified by a composite ophiolitic belt surrounding the whole region. Opening and closing of these small oceanic basin were probably coupled with huge lateral displacements and block rotations (Mattei et al., 2015) along a complex system of intracontinental faults active with different kinematics at different times along the present-day Great Kavir - Doruneh Fault (Javadi et al., 2013, 2015). Central Iran is presently delimited to the north by the curved (from NE-SW to NW-SE trending) left-lateral Great Kavir - Doruneh Fault that interplays

with the dextral N-S faults delimiting the Lut, Tabas, and Yazd blocks; these faults were probably inherited by the Palaeozoic or even older evolution of the region (Berberian and King, 1981). Complex interactions among these crustal scale wrench systems play a fundamental role in the present-day setting of the whole area (Calzolari et al., 2016), as well as in its past evolution.

2.1 The closure of the Palaeotethys and its implications for Central Iran

The closure of the Palaeotethys and the consequent Cimmerian Orogeny in Iran have been the subject of several researches (Berra et al., 2007; Horton et al., 2008; Fürsich et al., 2009; Zanchi et al., 2009a; Zanchetta et al., 2009). Palaeogeographic reconstructions agree upon the drift of the Iran microplate from Gondwana during the Early Permian (Sengör, 1979; Berberian and King, 1981; Stampfli et al., 1991; Dercourt et al., 2000; Stampfli and Borel, 2002; Torsvik and Cocks, 2004; Angiolini et al., 2007), and its docking to the southern active margin of Eurasia in the Late Triassic. In alternative, Golonka (2004) suggests multiple collisions of the single blocks forming Iran between the Late Triassic and the Early Jurassic. Collision followed a long-living subduction of the Palaeotethys Ocean along a north-dipping subduction zone below the southern Eurasian margin, at least during the Carboniferous (Golonka and Gawęda, 2012). Evidence for this event is preserved all along northern Iran (Ruttner, 1993; Wilmsen et al., 2009;; Zanchi et al., 2009a).

Remnants of this subduction occur in the Talesh Mountains, western Alborz, as documented by the occurrence of the Carboniferous Shanderman eclogites (Zanchetta et al., 2009; Omrani et al., 2013). Around Mashhad, remnants of an accretionary wedge related to the Palaeotethys closure are known since a long time (Stöcklin, 1974; Alavi, 1991; Boulin, 1991; Ruttner, 1993; Alavi et al., 1997; Sheikholeslami and Kouhpeyma, 2012). In addition, east of Mashhad in the Fariman-Aghdarband region of NE Iran, the arc-related units of Fariman and Darreh Anjir also record active subduction during the Permian, as well as during Devonian and Carboniferous (Zanchetta et al., 2013, Moghadam et al., 2014). Finally, the arc-related succession of Aghdarband, exposed north of

Fariman also testifies to an active margin related to the Palaeotethys subduction during the Early to Middle Triassic (Ruttner, 1991; Zanchi et al., 2016).

The Late Triassic age of the Cimmerian event is constrained by the Upper Triassic to Lower Jurassic syn- to post-collisional deposits of the Shemshak Group (Alborz) and equivalent successions of the Kopeh Dagh and Central Iran (Horton et al., 2008; Fürsich et al., 2009; Wilmsen et al., 2009; Zanchi et al., 2009a, 2015). These successions unconformably cover both the deformed Gondwanan passive margin and the Eurasian marginunits.

This general scenario considers that the Palaeotethys subduction and the Cimmerian collisional orogen should occur along the northern margin of the Iranian plate. Nevertheless, subduction and collision-related units are also present in Central Iran, far from the Cimmerian units now exposed in North Iran. They are the Anarak and Jandaq Metamorphic Complexes (respectively AMC and JMC), as well as the Triassic arc-related Nakhlak succession and the Triassic Doshak and Bayazeh Flysch, that record a Carboniferous to Triassic accretionary history (Bagheri and Stampfli, 2008; Balini et al., 2009; Zanchi et al., 2009b; Zanchi et al., 2015). Based on palaeomagnetic data, Davoudzadeh et al. (1987) suggested that the "Variscan units" of- Central Iran are displaced fragments of the Palaeotethys suture from the present-day Afghan–Iranian border region, reaching their position after a 135° anticlockwise rotation of Central Iran (Soffel et al., 1996). Bagheri and Stampfli (2008) interpret these metamorphic units as part of the Palaeotethys suture originally placed east of Mashhad; they reached the present position due to the opening and subsequent closure of the Sabzevar Ocean during the Cretaceous, accompanying the anticlockwise rotation of Central Iran. Recently, new palaeomagnetic data (Mattei et al., 2015) show a maximum anticlockwise rotation up to 85° in Jurassic beds of Central Iran. These new data thus suggest an important role of vertical axis rotations, but less intense with respect to that proposed by Davoudzadeh et al. (1987), suggesting that other processes should be responsible for the present-day setting of Central Iran.

3. Stratigraphy

The upper Palaeozoic Godar-e-Siah Complex of Jandaq is exposed along the NW corner of the Jandaq Metamorphic Complex (JMC), immediately to the south of the Great Kavir – Doruneh Fault. The contact of the Palaeozoic succession with the JMC is not exposed, but it is likely tectonic in nature, according to available geological maps (Aistov et al., 1984) and stratigraphic considerations. The age and kinematics of the tectonic contacts is problematic, as this area, after the Cimmerian events, was strongly deformed, so that the present-day position of these outcrops may be considerably different from the original one.

The upper Palaeozoic Godar-e-Siah Complex of Jandaq is preserved as three unconnected, fault-bounded outcrops unconformably covered by Cretaceous and younger sediments (Fig. 2). Eocene plutonic and small subvolcanic bodies intruded the Palaeozoic beds and the overlying succession, further complicating the reconstruction of the original geometric relationships within the Godar-e-Siah Complex.

The three outcrops were considered by Aistov et al. (1984) and Bagheri and Stampfli (2008) as part of a single succession, reaching more than 1000 m in thickness. However, the absence of physical continuity among the exposed areas prevents direct correlations; as a consequence, the interpretation of the Godar-e-Siah Complex as a single succession remains speculative.

The three outcrops, which are separately described below, are (Fig. 2): 1) the Godar-e-Siah northern outcrop; 2) the Godar-e-Siah central outcrop; 3) Chah Rizab (southwestern outcrop). The two southernmost outcrops are characterized by the dominance of carbonates (associated with volcanic rocks at Chah Rizab), whereas the the Godar-e-Siah northern outcrop essentially consists of siliciclastic deposits. The Godar-e-Siah northern outcrop, being better preserved and showing a greater stratigraphic continuity, is described in more details.

3.1 Godar-e-Siah northern outcrop

This well-exposed and poorly deformed succession consists of metric alternations of conglomerates, reddish to greenish sandstones and siltstones with rarer fossiliferous limestones in the uppermost part (Fig. 3). The succession crops out between Eocene volcanic hypabyssal rocks (porphyritic monzonites; Aistov et al., 1984) at the base and Cretaceous carbonates at the top. The upper contact is tectonic, whereas the lower one is not defined due to poor exposure (likely intrusive, may be tectonically reactivated).

Several m-thick porphyritic dikes and hypabyssal bodies intrude the succession: these dikes show strong lithological similarities with the Eocene volcanic rocks that are in contact with the studied succession, suggesting a coeval emplacement.

The clastic succession is tilted up to 65°, but its primary features are perfectly preserved due to the absence of the strong deformation that affects the other Palaeozoic outcrops in the Jandaq area.

Aistov et al. (1984) described this succession and reported a Lower Permian fossiliferous bed in its upper part. However, the four brachiopod species listed by Aistov et al. (1984, p. 46) comprise Pennsylvanian (not Lower Permian) taxa. Bagheri and Stampfli (2008) interpreted this succession as lacustrine evolving to paralic/littoral conditions, and reported the presence of one Pennsylvanian fusulinid taxon (*Montiparus*) with Eurasian affinity. The authors dated this succession as Upper Carboniferous-?Permian, even if they had no evidence for a Permian age.

In order to clarify the age and stratigraphic setting of this succession, we measured a complete stratigraphic section about 300 m-thick (Fig. 4), and collected samples for biostratigraphic and petrographic characterization. The succession (Figs 3, 4) consists of an alternation of m-thick beds of conglomerates with a sharp base, locally erosional, and sandstones with rare siltstones and carbonates. The conglomerate beds often show a lenticular shape and are interpreted as channel fills. Selection is poor; clasts in the conglomerates (up to 25 cm in size) are generally rounded and consist of volcanic rocks, cherts, limestones (recrystallized bioclastic limestones with crinoids, resembling those occurring in the Chah Rizab and Godar-e-Siah Central outcrops), and marble.

Conglomerate beds are abundant in the middle part of the succession, suggesting a coarsening upward trend in the lower part of the unit, followed by a fining upward trend in the upper part.Carbonate nodules (probably calcrete) occur in the sandy and silty facies (frequently reddish in the lower part of the succession). Toward the top of the succession, marine conditions are documented by a m-thick horizon of sandy limestones containing a rich assemblage of brachiopods (see paragraph 4.3), crinoids, bryozoans and corals (Fig. 5). Above this interval, sandstones with cross lamination (locally herringbone), that suggest deposition in tidal settings, dominate the upper part of the unit. The overall trend of the succession is fining-upward, with a higher textural maturity in its upper part.

The aggradational trend of the succession suggests a continuous creation of accommodation space, with a transgressive trend documented by the transition from continental to transitional and shallow-marine environments. The facies association together with the sedimentary structures suggest an alluvial plain depositional environment evolving to a coastal setting in the middle-upper part of the succession.

Above this unit, Aistov et al. (1984) described 350-400 m of unfossiliferous sandstones and siltstones preserved as separate outcrops within the Eocene intrusives. This part of the succession was not investigated during our fieldwork.

3.2 Godar-e-Siah Central outcrop

The Palaeozoic succession, here strongly deformed and faulted (Fig. 2), is unconformably covered by Cretaceous conglomerates and intruded by Eocene andesitic dikes and hypabyssal bodies. Due to intense deformation, the outcrop consists of a jigsaw of different types of rocks (Fig. 6), folded and displaced by a net of faults, so that it is extremely complex to define the original stratigraphic relationships in order to reconstruct a coherent stratigraphic succession. This complexity lead to different interpretations by previous authors. Aistov et al. (1984, fig. 11-I-III) described two separate sections: one consisting of Lower Carboniferous recrystallized limestones capped by

metasandstones; the other comprising metasandstone followed by Upper Carboniferous coral and crinoidal limestones and finally by sandstones. Instead, Bagheri and Stampfli (2008) interpreted this succession as made of platform to slope deposits of Middle to Late Carboniferous age. However, the fossils they figured (Bagheri and Stampfli, 2008, pl. 1-N, pl. 2-D) are all of Late Carboniferous (=Pennsylvanian) age.

Based on our new investigations, the main types of rocks here identified are: i) siltstones and sandstones, ii) bedded limestones (locally cherty) with marlstones and iii) massive limestones.

The siltstones and sandstones, frequently associated with thin layers of yellowish carbonates, show intensive folding. The mixed calcareous-siliciclastic succession consists of dominating well-bedded dark limestones. In the lower part of the succession, the unit includes dark bedded cherty limestones. The bedded limestones, characterized by the presence of marly interlayers, pass to burrowed (with horizontal, unlined, unbranched curved burrows, possibly *Planolites*) limestones rich in crinoids and probably phylloid algae. Above this interval, dark, bedded limestones alternating with marly limestones, marlstones and thin sandstone layers, contain brachiopods (see paragraph 4.3) and abundant solitary corals. This succession, preserved only in the central part of the outcrop, is in tectonic contact with massive limestones that contain abundant bryozoans.

According to the observed facies assemblages, the succession was deposited in a low-lattude (tropical) setting. The presence of marlstones with rare sandstones and the dominance of carbonates with intense burrowing, and with brachiopods, crinoids, solitary corals and bryozoans indicate deposition in subtidal settings. The occurrence of massive limestones with bryozoans confirms shallow water conditions, whereas cherty limestones suggest deposition in a deeper setting.

3.3 Chah Rizab outcrop

It is an isolated rocky spur within recent deposits and bordered to the east by a fault, which separates it from the metamorphic basement of the JMC. The succession mainly consists of deformed fine-grained volcanoclastic/pyroclastic deposits associated with strongly sheared and

recrystallized lenses of massive limestones (Fig. 7). Undeformed andesitic dikes, likely Cenozoic in age, crosscut the succession. The carbonate lenses contain crinoid ossicles and rare, poorly preserved, brachiopods. Deposits with scattered, unselected carbonate lithic clasts embedded in a volcanic matrix reflect possible explosive volcanic events. The post-depositional deformation prevents the reconstruction of the geometry of the succession, so that it is impossible to evaluate its thickness. However, Aistov et al. (1984) reported a 325-390 m-thick volcanoclastic succession of Mississippian age based on the presence of brachiopods. Bagheri and Stampfli (2008) described pyroclastic deposits with sandstones, Upper Devonian-Tournasian coral and crinoidal limestones and Lower Devonian marbles, which they interpreted as reworked olistoliths.

Southward, poorly selected, coarse conglomerates and sandstones (Unit 3 of Bagheri and Stampfli, 2008) unconformably cover this succession (Fig. 7). Clasts consist of rare Palaeozoic limestones (comparable to those underlying the conglomerates), metamorphic rocks and prevailing cobbles and boulders (up to 1 m in size) of different types of magmatic rocks, mostly granitoids, sampled for radiometric dating (U/Pb on zircons). Bagheri and Stampfli (2008) reported the presence of serpentinite clasts but we could not find evidence of it in the field. Sedimentological observations document poor selection, low textural and compositional maturity suggesting deposition by mass flows in a continental setting close to the source area, where intrusive, carbonate and metamorphic rocks were exposed. Bagheri and Stampfli (2008, p.129) argued a possible Visean age of the conglomerates based on the occurrence of Visean foraminifera within reworked, deformed carbonate clasts. Accordingly, an age younger than the Visean is more likely.

4. Analytical results

In order to clarify the stratigraphic relationships among the three studied outcrops, we constrained their sediment composition and provenance, their age and the palaeobiogeographic affinities of the preserved fauna, as described in the following paragraphs.

4.1 Sandstone petrography

Nine thin sections from samples collected along the measured stratigraphic section at the Godar-e-Siah northern outcrop (Tab. 1) were analysed and points-counted by the Gazzi-Dickinson method, modified to collect full information on each encountered rock-fragment type (Ingersoll et al., 1984; Garzanti and Vezzoli, 2003). Sandstones (Fig.4, 8) were classified by their main components exceeding 10%QFL (e.g., in a quartzo - feldspatho - lithic sandstone L > F > Q > 10%QFL).

In the lower part of the Godar-e-Siah northern outcrop, sandstones range from feldspatholithoquartzose volcaniclastic to lithoquartzose sedimentaclastic (samples from AJ60 to AJ70; Fig. 9). Sandstones are from poorly to moderately sorted with low-spherical, subangular to poorly rounded grains. They commonly consist of volcanic monocrystalline and polycrystalline quartz, sericitized plagioclase, chert and cherty shale, felsitic volcanic and microlitic grains, volcanic quartz-bearing rhyolitic grains and rare biotite and few low-grade metapsammite-metapelite metamorphic rock fragments. A few red spinels also occur.

In the upper part of the unit, the compositional maturity increases and sandstones range from lithoquartzose volcaniclastic to quartzose (samples from AJ72 to AJ80; Fig. 8, 9). Sandstones are poorly to moderately well-sorted with low-sphericity poorly rounded to subangular grains. This part of the succession is characterized by volcanic monocrystalline quartz and few sericitized plagioclase. Rock fragments are mainly volcanic quartz-bearing rhyolitic and microlitic grains with plagioclase, few felsitic volcanic and subordinately microlitic grains with plagioclase. Chert and cherty shale are common, with rare granitoid and aplitic rock fragments.

Detrital modes plotted into the log-ratio binary diagram (Fig. 9a) have a semiquantitative weathering index (*wi*; Weltje, 1994) from 0 to 2, indicating a compositional range from low to medium degrees of weathering. The *wi* is founded on quartz, feldspars and lithic fragments and, because it is based only on modern sediments, post-sedimentary processes (e.g. diagenesis) have to be considered. In fact, diagenetic modifications reduced feldspars and lithic fragments and thus shifted the composition to higher quartz contents and, consequently, higher weathering indices.

However, the observed low-medium weathering indices cannot be explained by post sedimentary processes only, but by provenance and the evolution of the sedimentary environments. Sandstones composition should resemble the primary mineralogy of sediments defined by the source rocks and the increase of the compositional maturity toward the top confirm the observed transition from alluvial to coastal depositional settings (Fig.9b). The compositional trend with the progressive increase of quartz at the expense of volcanic lithic grains, recorded by terrigenous sequences deposited in the Godar-e-Siah northern outcrop, thus highlights the erosion of a magmatic arc. (*Dissected Magmatic Arc Provenance*; Fig. 9c; Dickinson 1985; Garzanti and Andò 2007).

4.2 Geochronology

We processed three samples for zircons separation: one granite boulder (AJ42) in the conglomerate covering the limestone and the volcanic deposits in the Chah Rizab outcrop (Tab. 1 for sample location), a granodiorite clast in the conglomerate from the Godar-e-Siah northern outcrop (sample AJ52), and a dike (AJ56) that crosscuts the conglomerates.

4.2.1 Analytical methods

Zircon separation was carried out by standard heavy liquid and magnetic techniques. Zircon grains were then selected by handpicking under a petrography microscope, mounted in epoxy and polished. SHRIMP II U-Pb isotopic analyses were performed at the Beijing SHRIMP Center, Institute of Geology (CAGS, Beijing). Operating conditions and data acquisition were as described by Compston et al. (1992) and Williams (1998 and reference therein). Spot size was ~20 μm. 120-200 s of primary beam pre-sputtering was performed on each spot to remove common Pb on the surface, or contamination from gold coating. Inter-element fractionation and U concentration were controlled using Temora (416.8 ± 1.1 Ma; Black et al., 2003) and M257 (561.3 ± 0.3 Ma, U ~ 840 ppm, Th/U ~ 0.27; Nasdala et al., 2008) zircons standards, respectively. The analyses were corrected for common Pb using measured ^{204}Pb following Williams (1998). The common Pb

composition was obtained according to the Stacey and Kramers (1975) model. The ^{235}U decay constant used for age calculation is after Schöne et al. (2006), whereas the ^{238}U one is after Steiger and Jäger 1977. Analytical data were processed with Squid 1.02 (Ludwig, 2003b) and Isoplot (Ludwig, 2003a). Analytical data are reported in Tab. 2. Errors given for individual analyses are at 1σ level. Due to the systematic loss of ^{207}Pb signal during in-situ analysis of Neoproterozoic and younger zircons we did not report in Tab. 2 the systematic reverse discordant ages of such spots. For ages >1800 Ma the preferred age (italics in Tab. 2) is $^{207}Pb/^{206}Pb$, whereas for younger ages is $^{206}Pb/^{238}U$.

4.2.2 Results

Sample AJ42 is a boulder of pink coloured porphyry granite with a sub-hypabyssal texture made of quartz, K-feldspar, plagioclase, biotite and accessory minerals like zircon, apatite and oxides. Forty-five zircons grains were obtained from separation procedures. The zircon population displays a significant variety in both size and morphology. Size ranges from 70 to 200 μm with most of the grains being around 100-120 μm. Zircons are generally subeuhedral with some prismatic crystals. Rounded grains also occur, that likely represent inherited xenocrysts affected by resorption. The age patter is complex with zircons showing U-Pb ages ranging from Carboniferous to Neoarchean (Tab. 2 and Fig. 10d). Five among 22 spots are discordant (Tab. 2), so we did not consider them for the interpretation. The remaining 17 analyses span over a large range of concordant ages from 353.3 ± 1.6 to 2657 ± 9 Ma. 4 analytical spots (AJ42-3.2c, AJ42-4.2c, AJ42-5.1r, AJ42-8.2r, Tab. 2) provide concordant ages from 353.3 ± 1.6 to 355.1 ± 1.3 Ma (Tab. 2) with a weighted average mean of 354.3 ± 1.8 Ma (Fig. 10a) that has been interpreted as the crystallization age of the granite from which the pebble derives. Two spots (AJ42-3.2c and AJ42-4.2c) were focused on bright CL euhedral cores with oscillatory growth zoning, over which a dark rim with similar oscillatory zoning (Tab. 2) is overgrown. These darker rims provided discordant ages in two cases (spot AJ42-

3.1r and AJ42-4.1r, Tab. 2), whereas they display concordant ages (spot AJ42-5.1 and AJ42-8.2) identical within errors to the core ages described above.

The other dated zircons fall in two age intervals: i) 560-850 Ma; ii) 1810-2680 Ma. Neoproterozoic ages were obtained from euhedral to subheuedral zircons, most of them displaying a magmatic oscillatory zoning, both within cores and rims. Neoarchean ages were obtained from rounded grains or cores displaying uniform bright luminescence or a fading zonation of possibly metamorphic origin.

Sample AJ52 is a cobble made of grey-pink granodiorite, which lacks any evidence of solid-state deformation. The granodiorite is medium grained and consists of quartz, K-feldspar, plagioclase, biotite, rare amphibole and accessory minerals. 20 zircon grains were separated from the crushed sample but only few of them were suitable for U-Pb isotope analysis due to the occurrence of fractures, metamictization processes or growth domains too small to be analyzed. Seven concordant ages have been obtained (Tab. 2, Fig. 10b). One single rounded zircon provides a Neoproterozoic age (646.4 ± 4.1 Ma, spot AJ52-4.1c), whereas other analyzed zircons fall in the late Devonian to Mississippian time interval (Tab. 2 and Fig. 10e). Late Devonian ages (374 ± 1.7 to 371.2 ± 2.1 Ma) have been obtained from zircon cores displaying oscillatory zoning (Fig. 10b) and systematically associated to zircon rims with Mississippian ages (358.9 ± 1.5 and 357.4 ± 3.0 Ma, Fig. 10b). Zircon core and rim ages span a time interval of 15-20 Ma with no evidence of cores corrosion before rims growth. Following these observations, we suggest that the cores possibly represent former xenocrysts that remain in equilibrium with the melt in the magmatic chamber before the final crystallization of the granodiorite occurred in the Mississippian.

Sample AJ56 derives from the porphyry monzonites dated by Aistov et al. (1984) that intrudes the Godar-e-Siah Carboniferous conglomerates. About 60 zircons grains were separated from the crushed sample and 25 analytical spot were performed on them (Tab. 2). The age distribution displays a complex age pattern with youngest zircons having an early Eocene age and oldest grains reaching the late Palaeoproterozoic ages (Tab. 2). Seven spot performed on rims of large (120-180

μm, Fig. 10c) nearly equant zircon prisms provided concordant analyses in the 52.3 ± 0.5 – 58.8 ± 1.6 Ma time interval across del Palaeocene-Eocene boundary, with a weighted average $^{206}Pb/^{238}U$ age of 53.01 ± 0.4 (Fig. 10c). We interpret this age as the dike intrusion age. A porphyry monzodiorite from the same complex gave a K/Ar age of 54 Ma (Aistov et al., 1984).

The age distribution (Fig. 10f) of older spot ages of sample AJ56 comprises Early Cretaceous (111.7 ± 0.4 and 118.1 ± 1.4 Ma), Middle Jurassic (167.6 ± 2.0 and 184.8 ± 0.8 Ma), Late Triassic (204.7 ± 1.4 Ma), Permian (252.9 ± 3.7 and 285.9 ± 4.4 Ma), Ordovician to Cambrian (427.9 ± 3.8 to 530.5 ± 1.6 Ma) and, finally, a single zircon grain with a Palaeoproterozoic age (AJ56-21.1c,1832 ± 5 Ma, Tab. 2). The complex age pattern obtained from AJ56 likely suggests crustal recycling of metamorphic and magmatic rocks linked to multiple orogenic events.

4.3 Biostratigraphy

Brachiopods (Fig. 11) have been collected from the Godar-e-Siah northern outcrop (samples AJ 58, AJ77) and the Godar-e-Siah central outcrop (samples AJ36, AJ37, AJ39, AJ90) (Tab. 1). Instead, samples treated for conodonts (AJ44 in the Chah Rizab outcrop, AJ59 in the the Godar-e-Siah northern outcrop) resulted sterile. In the Godar-e-Siah northern outcrop, the faunal association is quite diverse, despite its occurrence in a m-thick interval only. Brachiopods (Fig. 11; *Cleiothyridina* sp., *Choristites* aff. *C. mosquensis* Buchman, 1908, *Choristites* sp., *Orulgania* sp.), smaller foraminifers, and fusulinids (Fig. 12; *Bradyina* cf. *B. magna* Roth and Skinner, 1930, *Bradyina nautiliformis* Rauzer-Chernousova and Reitlinger in Rauzer-Chernousova and Fursenko, 1937, *Pseudoacutella grozdilovae* (Maslo and Vachard, 1997) emend. Vachard et al., 2013, *Ozawainella* sp., *Neostaffella ozawai* (Lee and Chen in Lee et al., 1930), *Moellerites paracolaniae* (Safonova in Rauzer-Chernousova et al., 1951), *Profusulinella* (*Ovatella*?) sp. and *Eoschubertella/ Schubertellina* sp.) indicate a Moscovian (Kashirian) age for the fossiliferous horizon (Rauzer-Chernousova et al., 1951; Wagner et al., 1979; Leven, 1998; Leven et al., 2006; Gaetani et al., 2009; Leven and Gorgij, 2008, 2011; Davydov et al., 2010, Vachard et al., 2013). In the Godar-e-

Siah central outcrop, the brachiopods are less abundant and they are poorly preserved: the presence of *Deltachania* sp., *Choristites* aff. *C. mosquensis* and *Orulgania* sp. in the bedded limestones of the Godar-e-Siah central outcrop suggests a Pennsylvanian age also for these beds.

4.4 Palaeobiogeography

Fusulinids and brachiopods are mostly similar to assemblages from Spain, Russia, Kazakhstan, Siberia, China, North Thailand, Japan and Canada, indicating a North Palaeotethyan affinity.

Of the few brachiopod taxa recorded, *Cleiothyridina* is cosmopolitan, but *Deltachania* and *Orulgania* are only known from the north Palaeotethyan and Boreal regions, the former from Canada (Bamber and Waterhouse, 1971) and the latter from Kazakhstan, Siberia, N China, Canada, and Spain (e.g. Solomina and Cherniak, 1961; Grigorjeva, 1977; Martinez Chacon, 1978). In addition, the species *C. mosquensis* occurs in Uzbekistan, Kazhakstan, Russia, Siberia, North and South China, Canada, and Japan (e.g. Sarytcheva, 1960; Wagner et al., 1996; Chen and Shi, 2002).

This brachiopod association is quite distinctive and it has not been found in other Pennsylvanian fossil localities inCentral Iran (e.g.: Tabas and Anarak; Wendt et al. 2005). It is noteworthy that Pennsylvanian sedimentary successions and biota are quite rare both in Central and in Northern Iran, where the Permian succession unconformably lies on Devonian or Mississippian rocks (Wendt et al., 2002, 2005; Gaetani et al., 2009).

The recovered fusulinids are all known from the sedimentary successions of the East European Russian Platform (e.g.: western slope of the Urals, Moscow Basin, Volga region) (Rauzer-Chernousova et al., 1951; Grozdilova and Lebedeva, 1960; Grozdilova et al., 1975), the Canadian Arctic (Groves et al., 1994), the Indosinian part of North Thailand (Ueno and Igo, 1997), and the Akiyoshi area in Japan (Ozawa et al., 1992). Therefore, this assemblage is typical of the northern margin of the Palaeotethys.

In Iran, Gaetani et al. (2009) described a similar assemblage of fusulinids in the Qezel Qaleh Formation of the eastern Alborz. The two assemblages share the taxa *Ozawainella*, *Pseudoacutella*

grozdilovae and *Eoschubertella*; even *Moellerites* seems to be present - under the name of *Fusulinella*? sp. - in sample IR 942 of Gaetani et al. (2009, fig. 5.23-24). Both assemblages are late early Moscovian (Kashirian in age). Small differences in the association composition, i.e., the presence of *Hemifusulina* in the Godar-e-Siah northern outcrop and that of *Profusulinella* and primitive *Taitzehoella* in the eastern Alborz assemblage of Gaetani et al. (2009) can be explained by the slightly older age of the Godar-e-Siah assemblage (i.e., early/middle Kashirian vs. middle/late Kashirian).

5. Discussion

The integration of new data with the literature provides an improvement of the knowledge of the regional significance of the upper Palaeozoic succession of Jandaq, with implications on the reconstruction of the evolution of the Palaeotethys margins and the process of formation of the present-day Central Iran.

5.1 - Lithological data, age constraints and palaeobiogeographic affinities

Different lithological assemblages can be identified in the three distinct outcrops: volcanic rocks with subordinate marine carbonates at Chah Rizab, massive to bedded limestones and marlstones with minor siliciclastic intercalations in the Godar-e-Siah central outcrop and a completely different siliciclastic succession, mostly consisting of continental conglomerates and sandstones with rare fossiliferous marine intervals in the Godar-e-Siah northern outcrop.

At Chah Rizab, the newly obtained earliest Carboniferous radiometric ages (354 ± 1.8 Ma, Fig. 10) of the granitic cobbles contained in the conglomerates of the upper part of the succession confirm its post-Tournaisian age. A post-Visean age is documented by reworked carbonate blocks containing a Visean fauna (Bagheri and Stampfli, 2008).

In the Godar-e-Siah northern and central outcrops, in spite of the difference in lithological associtions, sedimentological features and deformation patterns, we found similar brachiopods

assemblages, which suggest the same Pennsylvanian age for both the successions. The age of the succession of the Godar-e-Siah northern outcrop was previously considered Late Carboniferous-Permian by Aistov et al. (1984) and Late Carboniferous-?Permian by Bagheri and Stampfli (2008). However, there is no evidence for a Permian age. Aistov et al. (1984) indicated an Early to Late Carboniferous age for the central Godar-e-Siah outcrop, which was otherwise considered Middle to Upper Carboniferous by Bagheri and Stampfli (2008). However, as said above, the fossils they reported are in fact Pennsylvanian only.

Our new data (from brachiopods and fusulinids) constrain the age of the northern outcrop to the Moscovian (Kashirian) and a similar age can be assumed for part of the central Godar-e-Siah outcrop, which shows the same brachiopod taxa (however, no fusulinids have been recorded from this area). Granodiorite pebbles collected in the Godar-e-Siah northern outcrop show radiometric ages very similar to the ones obtained at Chah Rizab. The occurrence of lithic clasts, both in the conglomerates of Chah Rizab and Godar-e-Siah northern outcrop, suggests that these clastic successions post-date an important tectono-magmatic event resulting in the intrusion, exhumation and erosion of arc-related magmatic rocks, their metamorphic basement, as documented by the sandstone petrography. This magmatic arc, according to our new dating, was active during the end of the Devonian and the beginning of the Carboniferous, preceding of about 20 My the metamorphism recorded in the Jandaq and Anarak Metamorphic complexes. In this latter scenario, the amphibolite-facies metamorphic basement of the Jandaq Metamorphic Complex could have been part of the dismembered magmatic arc–orogenic wedge complex.

Constraints on the palaeogeographic position of this arc-related succession are provided by the palaeontological content of the Godar-e-Siah Complex of Jandaq that strongly supports a north Palaeotethyan palaeobiogeographic affinity. Fusulinids and brachiopods are mostly similar to fossil assemblages from Spain, Russia, Kazakhstan, Siberia, China, North Thailand, Japan and Canada, and are thus consistent with locating the Jandaq sedimentary succession along the northern margin of the Palaeotethys (Fig. 13).

It is noteworthy that Bagheri and Stampfli (2008) previously mentioned the north Palaeotethyan biotic affinity of the fossils contained in the Godar-e-Siah Complex. In their paper, one of us (D.V.) reported, as personal communication, the finding of two North Palaeotethyan markers: *Quasiendothyra kobeitusana* Rauzer-Chernousova, 1948 of latest Famennian age followed up-sequence by the primitive triticitid *Montiparus* (middle Kasimovian in age, base of the Lower Pennsylvanian). The latter, in our current opinion, resembles *Montiparus citreus* Leven and Davydov, 2001, which was described from Darvaz, a North Palaeotethyan region (Vachard 1980; Angiolini et al., 2016).

More puzzling is the similarity of the Godar-e-Siah fusulinids with those of the Qezel Qaleh Formation of the eastern Alborz (Gaetani et al., 2009), as it is known to have been located along the Gondwanan margin in Carboniferous times (e.g. Muttoni et al., 2009a; Bahrammanesh et al., 2011). However, the slightly younger age of the Qezel Qaleh association may suggest a delayed migration of the fusulinid taxa from the northern speciation centres (supposedly Perilaurentian) to the northern Gondwana margin, which fits very well in the biotic distribution and palaeocurrents model of Angiolini et al. (2007). The authors envisaged the existence of a narrow zonal barrier in the Palaeotethys Ocean at the time of the Carboniferous-Early Permian Gondwanan glaciation, with a warm subtropical surface current gyre redistributing northern Palaeotethyan taxa at tropical latitudes, whereas cold currents distributed cold biota along the Gondwanan margin at slightly higher southern latitudes. The biota of the Alborz Mountains could have benefitted of this warm gyre not only in the earliest Permian as suggested by Angiolini et al. (2007), but also in the Pennsylvanian as indicated by the the Qezel Qaleh association.

5.2 - Comparison with the upper Palaeozoic successions of Iran and surrounding regions

The complexity of the evolution of the succession of Jandaq is even more striking when it is compared with the classical Carboniferous succession of Iran. In south-eastern Iran (Kerman, Hutak, Kuhbanan) the Middle Devonian-Carboniferous succession is represented by the Sibzar

Dolomite (Middle Devonian), Bahram Formation (upper Givetian to Frasnian), Shishtu Formation [consisting of different subunits, Fammenian-early Tournasian in age (Wendt et al., 2002), and Sardar and Hutak formations (Mississippian). The Jamal Formation covers these units with an angular unconformity. The Shishtu Formation (Famennian/lower Tournaisian) is considered an equivalent of the Bahram Formation (Wendt et al., 2002). The Middle Devonian-Carboniferous succession consists of shallow marine fine-grained siliciclastics and carbonates, occasionally with fluvial sediments. Carbonate platforms (Hutak Formation) and nearshore siliciclastic facies (Zarand Formation, to the south of the carbonate platform) are present (Wendt et al., 2002). In this area, the occurrence of the major stratigraphic gap between the Permian Jamal Formation and the underlying Devonian to Mississippian succession is documented by palaeosoils, erosional surfaces and local angular unconformities.

Moving to the north in Central Iran, the Sibzar, Bahram, Shishtu and Sardar formations form the Ozbak Kuh Group in the Tabas area. In the Yazd, Ardakan and Anarak regions, Carboniferous carbonates are known as the Gachal Formation (Visean-Namurian in age). In the Alborz Mountains, the Devonian-Carboniferous succession is represented by the Khosh Yeilagh (Givetian-Tournasian, Jenny, 1977), Geirud and Mobarak formations (Mississippian to Early Pennsylvanian; Wendt et al. 2005). This succession records the evolution from fluvial and deltaic shelf facies to marine carbonate deposition lasting until the early Pennsylvanian, when continental deposits (caliche, bauxites) document a regressive trend. After a gap in the Pennsylvanian, sedimentation resumed with the deposition of the carbonate succession of the Lower Permian Jamal Formation (Wendt et al., 2005). Anorogenic basaltic flows of uncertain age occur in the Devonian-Carboniferous succession, but arc-related magmatic rocks have never been reported. In the Alborz area the succession is similar, with the deposition of sandy limestones (Geirud Formation, Late Devonian) covered by shelfal carbonates (Mobarak Limestone, Mississippian) with minor siliciclastic input (Qezel Qaleh Formation, Pennsylvanian). All these successions show a Gondwanan affinity and

have been interpreted as part of the southern passive margin of the Palaeotethys Ocean (Wendt et al., 2005; Gaetani et al., 2009).

Arc-related Permian successions emplaced on the active Eurasian margin north of the Palaeotethys suture have been recognized in the Fariman area (Zanchetta et a., 2013), where alternating carbonates and basaltic lava flows have been described in a drowning succession covered by deep water turbiditic sandstones. At Aghdarband, north of Fariman, the preservation of the Palaeozoic sedimentary succession is poor and the slightly metamorphosed Devonian-Carboniferous units (Ruttner, 1993; Zanchi et al., 2016) forming the basement of the Kopeh Dagh are separated by an important wrench zone from the Triassic arc-related deposits. Volcanic sandstones and volcanoclastic deposits associated to dacitic to andesitic dikes are intercalated with Upper Devonian limestones (Ruttner, 1991). In addition, Carboniferous (Tournasian) limestones cover a conglomerate unit containing Upper Devonian-Mississippian conodonts (Ruttner, 1993).

According to the presented data, the Jandaq succession has no stratigraphic and limited palaeobiogeographic affinities with the coeval succession of Central Iran and the Alborz, whereas it shows some similarities with the Palaeozoic successions of Fariman and Aghdarband. The succession at Jandaq significantly differs in terms of lithology from the Central Iran successions, mostly because it records a proximal siliciclastic input related to a nearby active margin, associated with Carboniferous metamorphism (Bagheri and Stampfli, 2008), pre-dating the deposition of the Pennsylvanian conglomerates.

Several lines of evidence support the interpretation of the succession of Jandaq as part of the active margin of Eurasia (Fig.14). The occurrence of an arc-related Mississippian magmatic activity is documented by granitic pebbles in the Pennsylvanian conglomerates, as well as deformation and metamorphism of Carboniferous age in the adjacent basement units (Bagheri and Stampfli, 2008). A north-Palaeotethyan affinity is documented by the recovered fusulinids and brachiopods. The Carboniferous HP-LT metamorphism of the Anarak Metamorphic Complex (Zanchi et al., 2015)

and the Triassic forearc succession of Nakhlak (Balini et al., 2009) can be framed in the same palaeotectonic setting that is the northern active margin of the Palaeotethys Ocean (Figg.13, 14).

5.3 Palaeotethys remnants in Iran and their emplacement in Central Iran

The Eurasian affinity of the Jandaq succession, comprised between the Great Kavir-Doruneh Fault (Fig.1) and the Palaeozoic-Triassic successions of Gondwanan affinity of the Yazd block, needs to be explained in the frame of the regional distribution of Gondwanan and Eurasian successions in Iran.

At present, evidence of an active Eurasian margin is preserved in the Mashhad-Fariman-Aghdarband area (NE Iran, Alavi, 1991; Alavi et al., 1997; Sheikholeslami and Kouhpeyma, 2012; Zanchetta et al., 2013; Moghadam et al., 2014; Zanchi et al., 2016), about 550 km E-NE of Jandaq. In NE Iran these rock associations consist of mafic-ultramafic intrusive rocks (Mashhad and Darreh Anjir areas), basalts, siliciclastic turbidites and minor limestones with an Early to Middle Permian age (Fariman area). The spatial and temporal coexistence of intrusive and volcanic rocks with different geochemical affinity along with the stratigraphic evolution of the succession suggest that the Fariman basin developed as a fault-controlled intra-arc basin in a supra-subduction setting during the Permian (Zanchetta et al., 2013). The Darreh Anjir mafic-ultramafic complex has instead a Devonian age (Moghadam et al., 2014) and likely represents the remnants of oceanic to transitional crust that formed within an intra- or back-arc basin above an active subduction zone. These features suggest that the active margin of Eurasia from Devonian to Permian times was the locus of an Indonesian-type accretion tectonics involving formation and disruption of continental magmatic arcs and intra- and/or back-arc basins.

Several authors (Alavi et al., 1997; Bagheri and Stampfli, 2008; Zanchi et al., 2009b; Balini et al., 2009) discussed a possible original proximity of the Triassic Nakhlak succession to the Mashhad-Fariman and Aghdarband areas. Zanchi et al. (2015), in their analysis of the evolution of the Anarak Metamorphic Complex (a large fragment of an upper Palaeozoic accretionary wedge located just

south of the Jandaq Complex), support the allochthony of the unit and its provenance from NE Iran as a faulted portion of the Palaeotethys suture zone.

Although most of the authors now agree on the Palaeotethyan affinity and thus the allochthony of these Palaeozoic units, the mechanism of block translation from their original position to the Central Iran is still a matter of debate. Davoudzadeh et al. (1987) were the first authors to postulate large-scale rotations of the whole Central Iran microplate. This idea was supported by Soffel et al. (1996), based on a large set of palaeomagnetic data suggesting a 135° counter-clockwise (CCW) rotation of Central Iran since the Triassic. In contrast, Muttoni et al. (2009a and 2009b) did not find any significant rotations along vertical axes in the Triassic of Nakhlak. New palaeomagnetic data collected by Mattei et al. (2012, 2015) on the Jurassic to Neogene successions of Central Iran confirm the occurrence of large post-Cimmerian CCW rotations up to 85° confined to the Lut, Tabas and Yazd blocks. According to these authors, this rotation occurred during two distinct events, respectively between the Late Jurassic and Early Cretaceous and after the Middle-Late Miocene.

According to several authors (Bagheri and Stampfli, 2008; Zanchi et al., 2009b, 2015; Rossetti et al., 2010), one of the causes of the rotation, also envisaged by Mattei et al. (2015), could have been the opening of the Sabzevar ocean along a Mesozoic precursor of the -Great Kavir - Doruneh Fault, which acted as a transform fault (Barrier and Vrielynck, 2008). This fault system, still active today with a left-lateral strike-slip motion, showed a dextral shear sense in pre-Pliocene times, as documented by Javadi et al. (2013; 2015) based on structural information from the fault zone. These observations suggest that a large dextral separation up to 280 km occurred between the Eocene and the Pliocene, when the Great Kavir - Doruneh Fault became a left-lateral strike-slip fault (Javadi et al., 2013). This horizontal separation could help to justify at least in part the present-day position of the Eurasian active margin successions now lying among the Gondwanan units of the Alborz and Central Iran.

6. Conclusions

The upper Palaeozoic Godar-e-Siah Complex of Jandaq (Central Iran) consists of different lithological assemblages, which show a stratigraphic evolution and petrographic composition significantly different from the typical upper Palaeozoic successions of Gondwanan affinity of Central Iran.

Two main inferences can be drawn from our data: 1) the occurrence of Pennsylvanian (Moscovian) North Palaeotethyan fossil assemblages in the Godar-e-Siah northern and central outcrops; 2) the evidence of a Mississippian arc-related magmatic activity, testified by granitoid pebbles of Tournaisian age at Chah Rizab and at the Godar-e-Siah northern outcrop and by the sandstone composition of the latter.

The integration of these new data with literature data (Bagheri and Stampfli, 2008; Balini et al., 2009; Zanchi et al., 2009b, 2015) suggests that the deposition of the Godar-e-Siah Complex could be framed in an active margin setting. Unroofing and erosion of a magmatic arc to its roots was largely coeval with the deposition of conglomerates and sandstones in the Chah Rizab and Godar-e-Siah northern outcrops. The magmatic arc was located along the southern margin of Eurasia above the subducting Palaeotethys; such margin was likely active from the very Late Devonian to the Triassic, testifying for a long-lasting tectonic evolution that eventually led to the accretion of the Iranian block to the Eurasian margin.

The present day position of the Jandaq succession, bracketed between the Great Kavir - Doruneh Fault and the Palaeozoic-Triassic successions of Gondwanan affinity of the Yazd block, is the consequence of post-Cimmerian movements/rotations along this long-living fault system. The opening and closure of the Sabzevar Ocean and the subsequent activity of the Great Kavir - Doruneh Fault probably caused the translation of the Jandaq succession from its original position along the southern active margin of Eurasia to the interior of Central Iran.

Our data support the interpretation of Central Iran as a composite terrane deriving from the progressive accretion of different terranes, which amalgamated during Mesozoic and Cenozoic times because of different geodynamic events.

AKNOWLEDGEMENTS

We want to thank the Geological Survey of Iran of Teheran, for providing invaluable help during fieldwork in Central Iran in the frame of a Memorandum of Understanding between the Geological Survey of Iran and the Department of Earth and Environmental Sciences of Milano-Bicocca University. The present project was funded by the PRIN2010-2011 (prot. 2010AZR98L_007) Italian MIUR project: "**Birth and death of oceanic basins: geodynamic processes from rifting to continental collision in Mediterranean and Circum-Mediterranean orogens".** The DARIUS PROGRAMME is also thanked for providing logistic help and stimulating scientific issues. We are grateful to Andrea Baucon for discussions about fossil traces. Finally, we wish to thank to anonymous reviewers and the editorial board for their helpful suggestions.

References

Agard, P., Omrani, J., Jolivet, L., Mouthereau, G., 2005. Convergence history across Zagros (Iran): Constraints from collisional and earlier deformation, International Journal of Earth Sciences 94, 401–419.

Aistov, L., Melnikov, B., Krivyakin, B., Morozov, L., 1984. Geology of the Khur area (Central Iran). Explanatory text of the Khur Quadrangle Map 1:250,000, 132 pp.

Alavi, M., 1991. Sedimentary and structural characteristics of the Paleo-Tethys remnants in northeaster Iran. Geological Society of American Bulletin 103, 983–992.

Alavi M., Vaziri H., Seyed Enami K., Lasemi Y., 1997. The Triassic and associated rocks of the Nakhlak and Aghdarband areas in central and northeastern Iran as remnants of the southern Turanian active continental margin. Geological Society of American Bulletin 109, 1563-1575.

Angiolini, L., Gaetani, M., Muttoni, G., Stephenson, M.H., Zanchi, A., 2007. Tethyan oceanic currents and climate gradients 300 my ago. Geology 35, 1071-1074.

Angiolini, L., Campagna, M., Borlenghi, L., Grunt, T., Vachard, D., Vezzoli, G., Vuolo, I., Worthington, J., Nicora, A., Zanchi, A., 2016. Brachiopods from the Cisuralian-Guadalupian of Darvaz, Tajikistan and implications for Permian stratigraphic correlations, Palaeoworld http://dx.doi.org/10.1016/j.palwor.2016.05.006.

Bagheri, S., Stampfli, G.M., 2008. The Anarak, Jandaq and Posht-e-Badam metamorphic complexes in central Iran: New geological data, relationships and tectonic implications. Tectonophysics 451, 123-155.

Bahrammanesh, M., Angiolini, L., Antonelli, A.A., Aghababalou, B., Gaetani, M., 2011. Tournaisian (Mississippian) brachiopods from the Mobarak Formation, North Iran. Geoarabia 16, 129-192.

Balini, M., Nicora, A., Berra F., Garzanti, F., Levera, M., Mattei M., Muttoni, M., Zanchi, A., Bollati, I., Larghi, C., Zanchetta, S., Salamati, R., Mossavvari, F., 2009. The Triassic stratigraphic succession of Nakhlak (central Iran), a record from an active margin. In: Brunet, M.F., Wilmsen, M., Granath, J.W. (Eds), South Caspian to Central Iran Basins. Geological Society of London Special Publications 312, 287-321.

Bamber, E. W., Waterhouse, J. B., Mamet, B. L., Ross, C. A., 1971. Carboniferous and Permian stratigraphy and paleontology, northern Yukon Territory, Canada. Bulletin of Canadian Petroleum Geology 19, 29-250.

Barrier E., Vrielynck B., 2008. Palaeotectonic maps of the Middle East, Atlas of 14 maps. CGMW/CCGM, Paris, France.

Berberian, M., King, G., 1981. Toward a paleogeographic and tectonic evolution of Iran. Canadian Journal of Earth Sciences 18, 210–265.

Berra, F., Zanchi, A., Mattei, M., Nawab, A., 2007. Late Cretaceous transgression on a Cimmerian high (Neka Valley, Eastern Alborz, Iran): A geodynamic event recorded by glauconitic sands. Sedimentary Geology 199, 189-204.

Black, L.P., Kamo, S.L., Allen, C.M., Aleinikoff, J.N., Davis, D.W., Korsch, R.J., Foudoulis, C., 2003. Temora 1: a new zircon standard for Phanerozoic U-Pb geochronology. Chemical Geology 200,155-170.

Boulin, J., 1991. Structures in Southwest Asia and evolution of the eastern Tethys. Tectonophysics 196, 211–268.

Calzolari, G., Della Seta, M., Rossetti, F., Nozaem, R., Vignaroli, G., Cosentino, D., Faccenna, C., 2016. Geomorphic signal of active faulting at the northern edge of Lut Block: Insights on the kinematic scenario of Central Iran. Tectonics 35, 76–102.

Chen, Z.Q., Shi, G.R., 2002. Late Carboniferous to Early Permian brachiopod faunas from the Bachu and Kalpin areas, Tarim Basin, NW China. Alcheringa 25, 293-326.

Compston, W., Williams, I.S., Kirschvink, J.L., Zhang, Z., Ma, G., 1992. Zircon U-Pb ages for the Early Cambrian time-scale. Journal of the Geological Society of London 149, 171-184.

Davydov, V. I., Crowley, J. L., Schmitz, M. D., Poletaev, V. I., 2010. High-precision U-Pb zircon age calibration of the global Carboniferous time scale and Milankovitch band cyclicity in the Donets Basin, eastern Ukraine. Geochemistry, Geophysics, Geosystems, 11, 1-22.

Dercourt, J., Gaetani, M., Vrielynck, B., Barrier, E., Biju-Duval, B., Brunet, M.F., Cadet, J.P., Crasquin, S., Sandulescu M. (Eds.), 2000. Atlas of Peri-Tethys Paleogeographical maps. 24 maps and explanatory notes. CCGM/CGMW, Paris.

Dickinson, W. R. 1985. Interpreting provenance relations from detrital modes of sandstones. *In* Zuffa, G. G., ed. Provenance of arenites. NATO Advanced Studies Institute Series 148. Dordrecht, Reidel, 333–361.

Dickinson, W.R., Suczek, C.A., 1979. Plate tectonics and sandstone compositions. American Association of Petroleum Geologists Bulletin 63, 2164-2182.

Domeier, M., Torsvik, T.H., 2014. Plate tectonics in the Late Paleozoic. Geoscience Frontiers 5, 303–350.

Fürsich, F.T., Wilmsen, M., Seyed-Emami, K., Majidifard, M.R., 2009. Lithostratigraphy of the Upper Triassic-Middle Jurassic Shemshak Group of northern Iran. In: Brunet, M.F., Wilmsen, M., Granath, J.W. (Eds), South Caspian to Central Iran Basins. Geological Society of London Special Publications 312, 129-160.

Gaetani, M., Angiolini, L., Ueno, K., Nicora, A., Stephenson, M.H., Sciunnach, D., Rettori, R., Price G.D., Sabouri, J., 2009. Pennsylvanian-Early Triassic stratigraphy in the Alborz Mountains

(Iran). In: Brunet, M.F., Wilmsen, M., Granath, J.W. (Eds), South Caspian to Central Iran Basins. Geological Society of London Special Publications 312, 79-128.

Garzanti, E., Vezzoli, G., 2003. A Classification of Metamorphic Grains in Sands Based on their Composition and Grade. Journal of Sedimentary Research 73, 830-837.

Garzanti, E., Andò, S., 2007. Plate tectonics and heavy-mineral suites of modern sands. *In* Mange, M., and Wright, D. eds. Heavy minerals in use. Developments in Sedimentology Series. Vol. 58. Amsterdam, Elsevier, 809-833.

Golonka, J., 2004. Plate tectonic evolution of the southern margin of Eurasia in the Mesozoic and Cenozoic, Tectonophysics, 381, 235-273.

Golonka, J., Gawęda, A. 2012. Plate tectonic evolution of the Southern margin of Laurussia in the Paleozoic. In: E. Sharkov (Ed.), Tectonics - recent advances, Rijeka. InTech, 261-282.

Grigorjeva, A.D., 1977. Gladkosinusnye Spiriferidy verknego paleozoya Sibiri i Arktiki [Upper Paleozoic smooth-sinus spiriferids from Siberia and the Arctic], in Brakhiopody verkhnego paleozoya Sibiri i Arktiki [Upper Paleozoic brachiopods of Siberia and the Arctic]. Akademiya Nauk SSSR, Trudy Paleontologicheskogo Instituta 162, 37-54

Groves, J.R., Nassichuk, N.W., Rui Lin, W.W., Pinard, S. 1994. Middle Carboniferous fusulinacean biostratigraphy, northern Ellesmere Island (Sverdrup Basin, Canadian Arctic archipelago). Geological Survey of Canada Bulletin 469, 1-55.

Grozdilova, L.P., Lebedeva, N.S., 1960. Foraminifery kamennougolnykh otlozhenii zapadnogo sklona Urala i Tamana (Foraminifers of the Carboniferous deposits of western slope of Urals and Timan). Trudy VNIGRI 150, 1-264 (in Russian).

Grozdilova L.P., Lebedeva, N.S., Lipina, O.A., Malakhova, N.P., Mikhailova, Z.P., Chermnykh, V.A., Postoyalko, M.V., Simonova, Z.G., Sinitsyna, Z.A., Shcherbakova, M.V., 1975. Foraminifery (Foraminifera). In: Stepanov, D.L., Krylova, A.K., Grozdilova, L.P., Pozner, V.M., Sultanaev,

A.A., Paleontologicheskii atlas kamennougolnykh otlozhenii Urala (Paleontological atlas of the Carboniferous deposits from Urals). Izdateltsvo "Nedra", Trudy VSEGEI 383, 27-64 (in Russian).

Horton, B.K., Hassanzadeh, J., Stockli, D.F., Axen, G.J., Gillis, R.J., Guest, B., Amini, A., Fakhari, M.D., Zamanzadeh, S.M., Grove, M., 2008. Detrital zircon provenance of Neoproterozoic to Cenozoic deposits in Iran: Implications for chronostratigraphy and collisional tectonics. Tectonophysics 451, 97-122.

Ingersoll, R.V., Bullard, T.F., Ford, R.L., Grimm, J.P., Pickle, J.D., Sares, S.W., 1984. The effect of grain size on detrital modes: a test of the Gazzi-Dickinson point- counting method: Journal of Sedimentary Petrology 54, 103-116.

Javadi, H.R., Esterabi Ashtiani, M., Guest, B., Yassaghi, A., Ghassemi, M. R., Shahpasandzadeh, M., Naeimi, A., 2015. Tectonic reversal of the western Doruneh Fault System: Implications for Central Asian tectonics. Tectonics 34, 2034-2051.

Javadi, H.R., Ghassemi, M.R., Shahpasandzadeh, M., Guest, B., Ashtiani, M.E., Yassaghi,A., Kouhpeyma M., 2013. History of faulting on the Doruneh Fault System: implications for the kinematic changes of the Central Iranian Microplate. Geological. Magazine 150, 651-672.

Jenny, J.G., 1977. Géologie et stratigraphie de l'Elbourz oriental entre Aliabad et Shahrud, Iran. PhD thesis, Université de Genéve 238 pp.

Lee, J.S., Chen, S., Chu, S., 1930. The Huanglung Limestone and its fauna. Academia Sinica, Memoirs of the National Research Institute of Geology 9, 85-143.

Leven, E.Ya., 1998. Stratigraphy and Fusulinids of the Moscovian Stage (Middle Carbonifèrous) in the Southwestern Darvaz (Pamir). Rivista Italiana di Paleontologia e Stratigrafia 104, 3–42.

Leven, E.Ya., Davydov, V. I., 2001. Stratigraphy and fusulinids of the Kasimovian and Upper Gzhelian (Upper Carboniferous) in the Southwestern Darvaz (Pamir). Rivista Italiana di Paleontologia e Stratigrafia 107, 3-46.

Leven, E. Ya., Davydov, V. I., Gorgji, M. N., 2006. Pennsylvanian stratigraphy and fusulinids of Central and Eastern Iran. Palaeontologia Electronica 9 (1) (10 MB).

Leven, E.Ya., Gorgij, M.N., 2008. New Fusulinids of the Moscovian Stage found in Iran. Stratigraphy and Geological Correlation, 16, 383-399 (English translation of Stratigrafiya. Geologicheskaya Korrelyatsiya 16, 40-56 (in Russian).

Leven, E.Ya., Gorgij, M.N., 2011. Fusulinids and Stratigraphy of the Carboniferous and Permian in Iran. Stratigraphy and Geological Correlation 19, 687-776.

Ludwig, K.R., 2003(a). A User's Manual for Isoplot/Ex 3: A Geochronological Toolkit for Microsoft Excel. Berkeley Geochronological Center, Special Publication 4.

Ludwig, K.R., 2003(b). SQUID 1.02: A User's Manual. Berkeley Geochronological Center, Special Publication 2.

Martinez Chacon, M.L., 1978. Syningothyridacea (Brachiopoda) del Carbonifero de la Cordillera Cantabrica (N de Espana). Trabajos de Geologia 10, 317-330.

Maslo, A., Vachard, D., 1997. Inventaire critique des Eostaffellinae (foraminifères) du Carbonifère. Revue de Micropaléontologie 40, 39-69.

Mattei, M., Cifelli, F., Muttoni, G., Zanchi, A., Berra, F., Mossavvari, F., Eshraghi, S.A., 2012. Neogene block-rotation in Central Iran: evidence from paleomagnetic data. Geological Society of America Bulletin 124, 943-956.

Mattei, M., Cifelli, F., Muttoni, G., Rashid, H., 2015. Post-Cimmerian (Jurassic-Cenozoic) paleogeography and vertical axis tectonic rotations of Central Iran and the Alborz Mountains. Journal of Asian Earth Sciences 102, 92-101.

Moghadam, H.S., Xian-Hua Li, X.-H. Xiao-Xiao Ling, X.-X., Stern, R.J., Zaki Khedr, M.Z., Chiaradia, M., Ghorbani, G., Arai, S., Tamura, A., 2014. Devonian to Permian evolution of the

Paleo-Tethys Ocean: New evidence from U–Pb zircon dating and Sr–Nd–Pb isotopes of the Darrehanjir–Mashhad "ophiolites", NE Iran. Gondwana Research, 28, 781-799.

Muttoni, M., Mattei, M., Balini, M., Zanchi, A., Gaetani, M., Berra, F., 2009a. The drift history of Iran from the Ordovician to the Triassic. In: Brunet, M.F., Wilmsen, M., Granath, J.W. (Eds), South Caspian to Central Iran Basins. Geological Society of London Special Publications 312, 7-29.

Muttoni, G., Gaetani, M., Kent, D. V., Sciunnach, D., Angiolini, L., Berra, F., Garzanti, E., Mattei, M., Zanchi, A., 2009b. Opening of the Neo-Tethys Ocean and the Pangea B to Pangea A transformation during the Permian. GeoArabia 14, 17-48.

Nasdala, L., Hofmeister, W., Norberg, N., Mattinson, J. M., Corfu, F., Dörr, W., Kamo, S. L., Kennedy, A. K., Kronz, A., Reiners, P. W., Frei, D., Kosler, J., Wan, Y., Götze, J., Häger T., Kröner, A., Valley, J.W., 2008. Zircon M257 - a homogeneous natural reference material for the ion microprobe U-Pb analysis of zircon. Geostandards and Geoanalytical Research 32, 247-265.

Omrani, H., Moazzen, M., Oberheansli, R., Tsujimori, T., Bousquet, R.,. Moayyed, M., 2013. Metamorphic history of glaucophane-paragonite-zoisite eclogites from the Shanderman area, northern Iran. Journal of metamorphic Geology 31, 791-812.

Ozawa, T., Watanabe, K., Kobayashi, F., 1992. Morphologic evolution in some schwagerinid and schubertellid lineages and the definition of the Carboniferous-Permian boundary. Studies in Benthic Foraminifera, Benthos' 90, Sendai 1990: 389-401, Tokai University Press.

Rauzer-Chernousova, D.M., 1948. Materialy k faune foraminifer kamennougolnykh otlozhenii, Tsentralnogo Kazakhstana (Materials for foraminiferal fauna from the Carboniferous deposits from central Kazakhstan). Akademiya Nauk SSSR, Trudy Instituta Geologicheskikh Nauk 66, geologicheskaya seriya 21, 1-66 (in Russian).

Rauzer-Chernousova, D.M., Fursenko, A.V., 1937. Opredelitel foraminifer neftenosnykh raionov SSSR (Determination of foraminifera from the petroliferous regions of the USSR). Glavnaya Redaktsya Gorno-Toplivnoi Literatury Leningrad, 1-315 (in Russian).

Rauzer-Chernousova, D.M., Gryzlova, N.D., Kireeva, G.D., Leontovich, G.E., Safonova, T.P., Chernova, E.I., 1951. Srednekamennougolnye fuzulinidy Russkoi Platformyi sopredelnykh oblastey (Fusulinides du Carbonifère moyen de la Plate-forme Russe et des régions voisines). Akademiya Nauk SSR, Institut Geologicheskikh Nauk, Ministerstvo Neftyanoy Promishlennosti SSSR, 1-380 (in Russian).

Rossetti, F., Nasrabady, M., Vignaroli, G., Theye, T., Gerdes, A., Razavi, M.H., Vaziri, H.M., 2010. Early Cretaceous migmatitic mafic granulites from the Sabzevar range (NE Iran): implications for the closure of the Mesozoic peri-Tethyan oceans in central Iran. Terra Nova 22, 26-34.

Rossetti, F., R. Nozaem, F. Lucci, G. Vignaroli, A. Gerdes, M. Nasrabadi, and T. Theye, 2015. Tectonic setting and geochronology of the Cadomian (Ediacaran-Cambrian) magmatism in Central Iran, Kuh-e-Sarhangi region (NW Lut Block). Journal of Asian Earth Sciences, 102, 24–44.

Roth, R., Skinner, J.W., 1930. Fauna of the McCoy Formation, Pennsylvanian of Colorado. Journal of Paleontology 4, 332-352.

Ruttner, A.W., 1991. Geology of the Aghdarband area (Kopet Dagh, NE-Iran). Abhandlungen der Geologischen Bundesanstalt 38, 7-79.

Ruttner, A.W., 1993. Southern borderland of Triassic Laurasia in north-east Iran. Geologische Rundschau 82, 110–120.

Sarytcheva T.G. 1960. Bryozoa, Brachiopoda. In ORLOV, Y. A. (ed.). Osnovi Paleontologii [Fundamentals of Paleontology], volume 7. Izdatel'stvo Akademiia Nauk SSSR, Moscow, 343 pp. [In Russian].

Schöne, B., Crowley, J.L., Condon, D.J., Schmitz, M.D., Bowring, S.A., 2006. Reassessing the uranium decay constants for geochronology using ID-TIMS U-Pb data. Geochimica et Cosmochimica Acta 70, 426-445.

Sengör, A.M.C., 1979. Mid-Mesozoic closure of Tethys and its implications. Nature 279, 590–593.

Sharkovsky M., Susov. M., Krivyakin B., 1984. Geology of the Anarak area (Central Iran). Explanatory Text of the Anarak Quadrangle Map 1:250000. Geological Survey of Iran, V/O "Tecnoexport" USSR Ministry of Geology Reports, 19.

Sheikholeslami, M.R., Kouhpeyma, M., 2012. Structural analysis and tectonic evolution of the eastern Binalud Mountains, NE Iran. Journal of Geodynamics 61, 23–46.

Soffel, H.C., Eftekhar-Nezhad, J., Hushmandzadeh, A., 1996. New palaeomagnetic data from Central Iran and a Triassic palaeoreconstruction. Geologische Rundshau 85, 293-302.

Solomina, R.V., Cherniak, G.E., 1961. Orulgania - new spiriferid genus from the Upper Paleozoic of the Arctic. Paleontologicheskii Zhurnal 3, 61-66. In Russian

Stacey, J.S., Kramers, J.D., 1975. Approximation of terrestrial lead isotope evolution by a two-stage model. Earth and Planetary Science Letters 26, 207-221.

Stampfli, G.M., Borel, G.D., 2002. A plate tectonic model for the Paleozoic and Mesozoic constrained by dynamic plate boundaries and restored synthetic oceanic isochrones. Earth Planetary Science Letters 196, 17–33.

Stampfli, G.M., Marcoux, J., Baud, A., 1991. Tethyan margins in space and time. Palaeogeography, Palaeoclimatology, Palaeoecology 87, 373–409.

Steiger, R.H., Jäger, E., 1977. Subcommission on geochronology: convention on the use of decay constants in geo- and cosmochronology. Earth and Planetary Science Letters 36, 359-362.

Stöcklin, J., 1974. Possible ancient continental margins in Iran. In: Burk, C.A., Drake, C.L. (Eds.), The Geology of Continental Margins. Springer-Verlag, Berlin, pp. 873–887.

Torsvik, T.H., Cocks, R.M., 2004. Earth geography from 400 to 250 Ma: a palaeomagnetic, faunal and facies review. Journal of the Geological Society of London 161, 555–572.

Ueno, K., Igo, H., 1997. Late Paleozoic foraminifers from the Chiang Dao area, northern Thailand. Geologic age, Faunal affinity, and paleobiogeographic implications. Proceedings of the International Congress Carboniferous and Permian 13, 339-358.

Vachard, D., 1980. Téthys et Gondwana au Paléozoïque supérieur; les données afghanes: biostratigraphie, micropaléontologie, paléogéographie. Documents et Travaux IGAL, Institut Géologique Albert de Lapparent, 2, 2 volumes: 1-463.

Vachard, D., Krainer, K., Lucas, S.G., 2013. Pennsylvanian (Carboniferous) calcareous microfossils from Cedro Peak (New Mexico, USA). Part 2: Smaller foraminifers and fusulinids: Annales de Paléontologie 99, 1-42.

Wagner, R.H., Higgins, A.C., Meyen, S.V., 1979. The Carboniferous of the USSR. Reports presented to the IUGS Subcommission on Carboniferous Stratigraphy at the 8th International Congress on Carboniferous Stratigraphy and Geology held at Moscow 1975. Yorkshire Geological Society, Occasional Publications 4, 1-22.

Wagner, R.H., Winkler Prins, C.F. Granados, L.F. (eds), 1996. The Carboniferous of the world volume III. The Former USSR, Mongolia, Middle Eastern Platform, Afghanistan, and Iran. IUGS Publication 3. Istituto Tecnologico GeoMinero de Espana, 529 pp.

Weltje, G.J., 1994. Provenance and Dispersal of Sand-sized Sediments: Reconstruction of Dispersal Patterns and Sources of Sand-sized Sediments by Means of Inverse Modelling Techniques. PhD dissertation, Utrecht University, Geologica Ultraiectina 121 pp.

Wendt, J., Kaufmann, B., Belka, Z., Farsan, N., Bavandpur, A.K., 2005. Devonian/Lower Carbonifeous stratigraphy, facies patterns and palaeogeography of Iran Part II. Northern and Central Iran. Acta Geologica Polonica 55, 31–97.

Wendt, J., Kaufmann, B., Belka, Z., Farsan, N., Karimi Bavandpur, A., 2002. Devonian/Lower Carboniferous stratigraphy, facies patterns and palaeogeography of Iran. Part I. Southeastern Iran. Acta Geologica Polonica 52, 129-168.

Wheterill, G.W., 1956. Discordant uranium-lead ages. Transactions of the American Geophysical Union 37, 320-327.

Williams, I.S., 1998. U-Th-Pb geochronology by ion microprobe. In: McKibben, M.A., Shanks, W.C. III, Ridley, W.I. (Eds): Applications of microanalytical techniques to understanding mineralizing processes. Reviews of Economy Geology 7, 1-35.

Wilmsen, M., Fursich, F.T., Taheri, J., 2009. The Shemshak Group (Lower–Middle Jurassic) of the Binalud Mountains, NE Iran: stratigraphy, depositional environments and geodynamic implications. In: Brunet, M.F., Wilmsen, M., Granath, J.W. (Eds), South Caspian to Central Iran Basins. Geological Society of London Special Publications 312, 175–188.

Zanchetta, S., Zanchi, A., Villa, I., Poli, S., Muttoni, G., 2009. The Shanderman eclogites: a Late Carboniferous high-pressure event in the NW Talesh Mountains (NW Iran). In: Brunet, M.F., Wilmsen, M., Granath, J.W. (Eds), South Caspian to Central Iran Basins. Geological Society of London Special Publications 312, 57-78.

Zanchetta, S., Berra, F., Zanchi, A., Bergomi, M., Caridroit, M., Nicora, M., Heidarzadeh, G., 2013. The record of the Late Palaeozoic active margin of the Palaeotethys in NE Iran: Constraints on the Cimmerian orogeny. Gondwana Research 24, 1237-1266.

Zanchi, A., Malaspina, N., Zanchetta, S., Berra, F., Benciolini, L., Bergomi, M., Cavallo, A., Javadi, H.R., Kouhpeyma, M., 2015. The Cimmerian accretionary wedge of Anarak, Central Iran. Journal of Asian Earth Sciences 102, 45-72.

Zanchi, A., Zanchetta, S., Balini, M., Ghassemi, M.R., 2016. Oblique convergence during the Cimmerian collision: Evidence from the Triassic Aghdarband Basin, NE Iran. Gondwana Research, 38, 149-170.

Zanchi, A., Zanchetta, S., Berra, F., Mattei, M., Garzanti, E., Molyneux, S., Nawab, A., Sabouri, J. 2009a. The Eo-Cimmerian (Late? Triassic) orogeny in north Iran. In: Brunet, M.F., Wilmsen, M., Granath, J.W. (Eds), South Caspian to Central Iran Basins. Geological Society of London Special Publications 312, 31-55.

Zanchi, A., Zanchetta, S., Garzanti, E., Balini, M., Berra, F., Mattei, M., Muttoni, G., 2009b. The Cimmerian evolution of the Nakhlak-Anarak area, central Iran, and its bearing for the reconstruction of the history of the Eurasian margin. In: Brunet, M.F., Wilmsen, M., Granath, J.W. (Eds), South Caspian to Central Iran Basins. Geological Society of London Special Publications 312, 261-286.

Figure captions

Fig.1: Simplified geological map of Central Iran (modified from Zanchi et al., 2015). The boxes to the south-west of Jandaq indicate the position of the maps in fig. 2.

Fig. 2 – Geological sketches of the three studied outcrops in the Jandaq area (the position is indicated by the three boxes in Fig. 1 south-west of Jandaq). Geology from Aistov et al. (1984) and from our original field observations.

Fig. 3 – Details of the Godar-e-Siah northern outcrop: a) position of the measured stratigraphic section; b) detail of the mid part of the succession (alternating sandstones and conglomerates); c) silty layers containing carbonate nodules (caliches?) capped by a lenticular sandy body (on the right); d) cross laminations in the upper part of the succession; e) conglomerate bed, with rounded cobbles (middle part of the succession); f) hummocky cross laminations in well-selected, quartz-rich sandstones in the upper part of the section.

Fig. 4- Stratigraphic section of the Pennsylvanian clastic succession, Godar-e-Siah northern outcrop. The calcareous fossiliferous interval in the upper part of the section records the first clear evidence of marine conditions.

Fig. 5 – Fossiliferous interval in the Godar-e-Siah northern outcrop: a) massive corals; b) accumulation of crinoid ossicles.

Fig. 6 – Details of the Godar-e-Siah central outcrop: a) view from west; the succession is cut by volcanic rocks (V) and unconformably covered by Cretaceous units (K); b) detail of the Palaeozoic succession; c) bedded cherty limestones; d) massive limestones in contact with bedded limestones;

e) crinoidal limestones; f) burrowing at the base of a limestone bed; g) bryozoans in the massive limestone of figure 6d; h) bioclastic limestones (phylloid algae? arrows). Abbreviations: V: volcanic rocks (Cenozoic?); K: Cretaceous; Pm: Palaeozoic massive limestones; Ps: Palaeozoic sandstones; Pb: Palaeozoic bedded limestones.

Fig. 7 - Chah Rizab outcrop: a) panoramic view of the outcrop, where the following lithological units can be identified: V: volcanic rocks with Devonian limestones (L), according to Bagheri and Stampfli, 2008); C: conglomerate with lower Mississippian granitoid clasts (see figure 7e); b) strongly deformed and recrystallized massive limestones; c) poorly preserved brachiopod; d) strongly deformed Palaeozoic limestone with crinoids ossicles, e) poorly-selected massive conglomerates (see figure 7a).

Fig. 8 - Representative photomicrographs of selected samples. Sample AJ60 is characterized by volcanic monocrystalline quartz (Q), sericitized plagioclase (pl), chert (ch) and felsitic volcanic grains (VFR). Sample AJ70 consists of monocrystalline quartz (Q), sericitized plagioclase (pl), chert and cherty shale (ch), and low-grade metapsammite-metapelite rock fragments (MRF). Volcanic quartz-bearing rhyolitic and microlitic grains with plagioclase (VRF) characterize sample AJ72. Sample AJ80 consists of monocrystalline quartz (Q) and chert (ch). All photos with crossed polars; all white bars for scale are 250 microns.

Fig. 9 – Composition of the sandstones of the Godar-e-Siah Northern outcrop. A) Bivariate log-ratio plot of the analysed samples. The result indicates a low-medium semi-quantitative weathering index for all samples (*wi* = 0-2). B) Evolution of detrital modes: sandstone composition range from feldspatholithoquartzose volcaniclastic - lithoquartzose sedimentaclastic (samples AJ60 - AJ70) to quartzose - lithoquartzose volcaniclastic (samples AJ76 - AJ80). The compositional maturity thus increases up-section (QFL-diagram by Dickinson and Suczek, 1979); C) The grey arrow highlights

the ideal compositional trend recorded by terrigenous sequences accumulated in forearc and other arc-related basins during unroofing of the arc massif (Dickinson and Suczek, 1979).

Fig. 10 – a) Concordia diagram (Wheterill, 1956) of SHRIMP U-Pb analyses performed on sample AJ42 with ages younger than 1.0 Ga. Individual error ellipses are at 2σ level here and in the other Concordia diagrams. Error bars in the weighted average age diagram are also at 2σ level. MSWD: Mean Square of Weighted Deviates; Prob.: Probability of fit. The weighted average age from the four youngest spots is 354 ± 1.8 Ma and it is interpreted as the crystallization age. b) Concordia diagram of spot with ages younger than 400 Ma of sample AJ52. Zircon cores show Late Devonian ages, whereas rims with oscillatory zoning have ages younger of about 15-20 Myrs. c) Concordia diagram of sample AJ56, with $^{206}Pb/^{238}U$ ages younger than 240 Ma. The weighted average age of the seven youngest spots performed on large equant zircon prism is 53.0 ± 0.4 Ma and it is interpreted as the dike intrusion age. Relative probability diagram showing the distribution of concordant U-Pb zircon ages of samples AJ42 (d), AJ52 (e) and AJ56 (f), see text for discussion.

Fig. 11 – Brachiopods from the Godar-e-Siah northern and central outcrops: 1-2 *Cleiothyridina* sp. ind. AJ58-95; 3-5 *Deltachania* sp. ind. AJ90-11; 6-7 *Choristites* aff. *C. mosquensis* Buckman, 1908, AJ58-81; 8-9 *Choristites* aff. *C. mosquensis* Buckman, 1908, AJ58-31; 10 *Choristites* aff. *C. mosquensis* Buckman, 1908, AJ39b-12; 11 *Choristites* aff. *C. mosquensis* Buckman, 1908, AJ58-14; 12 *Choristites* sp. ind. AJ58-87; 13 *Choristites* sp. ind. AJ77-9; 14 *Orulgania* sp. ind. AJ39-4; 15-19 *Orulgania* sp. ind. AJ90-19. Scale bar is 1 cm.

Fig. 12 – Fusulinids from the Godar-e-Siah northern outcrop: 1-3 *Neostaffella* sp., AJ58; 4 *Bradyina nautiliformis*, Rauzer-Chernousova and Reitlinger in Rauzer-Chernousova and Fursenko, 1937 AJ77; 5 *Hemifusulina* sp., AJ77; 6 *Neostaffella ozawai* Rauzer-Chernousova and Reitlinger in Rauzer-Chernousova and Fursenko, 1937 and *Pseudostaffella* sp. (bottom, right), AJ77; 7 *Pseudoacutella grozdilovae* (Maslo and Vachard, 1997) emend. Vachard et al., 2013, AJ77; 8-11

Moellerites paracolaniae (Safonova in Rauzer-Chernousova et al., 1951), AJ77. Scale bar is 0.5 mm.

Fig. 13 – Pennsylvanian palaeogeography, at the time of deposition of the Jandaq successions. Modified from Domeier and Torsvik (2014). Warm equatorial currents in red, cold currents in blue. SG: presumed location of the Siah-e-Godar Complex, Tu: Turan, Af: Afghanistan; An: Annamia, Lh: Lhasa, Q: Qiangtang, Pa: S and Central Pamir with Karakoram, Ta: Taurides, Tr: Tarim, N-Ch: North China, S-Ch: South China.

Fig. 14 - Tentative paleogeographic reconstruction of the Palaeotethys at the time of deposition of the Palaeozoic Godar–e-Siah Complex of Jandaq. The sedimentary succession of the three isolated, fault-bounded fossiliferous carbonates, volcanics and siliciclastics deposits (Chah Rizab outcrop, the Godar-e-Siah northern outcrop, and the Godar-e-Siah central outcrop) is placed, according to the stratigraphic, structural, petrographic, palaeontological and geochronological investigations, along the southern margin of Eurasia during the subduction of the Palaeotethys Ocean, in a position that can be related to a backarc or forearc setting.

Table 1. Sample locations and analyses.

Table 2: SHRIMP U-Pb analytical data performed on zircons separated from samples AJ42, AJ52 and AJ56.

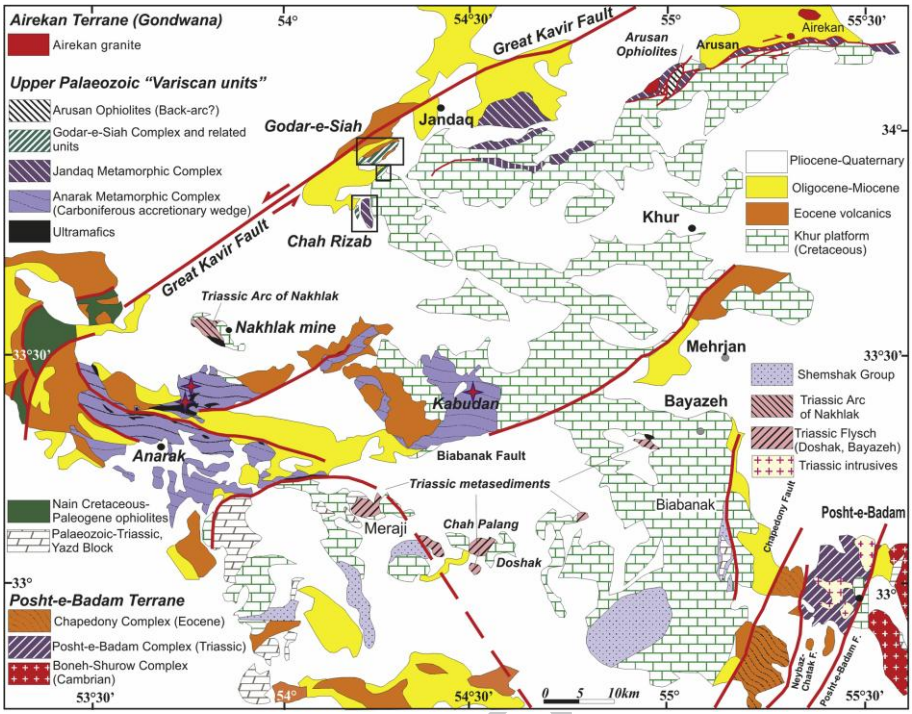

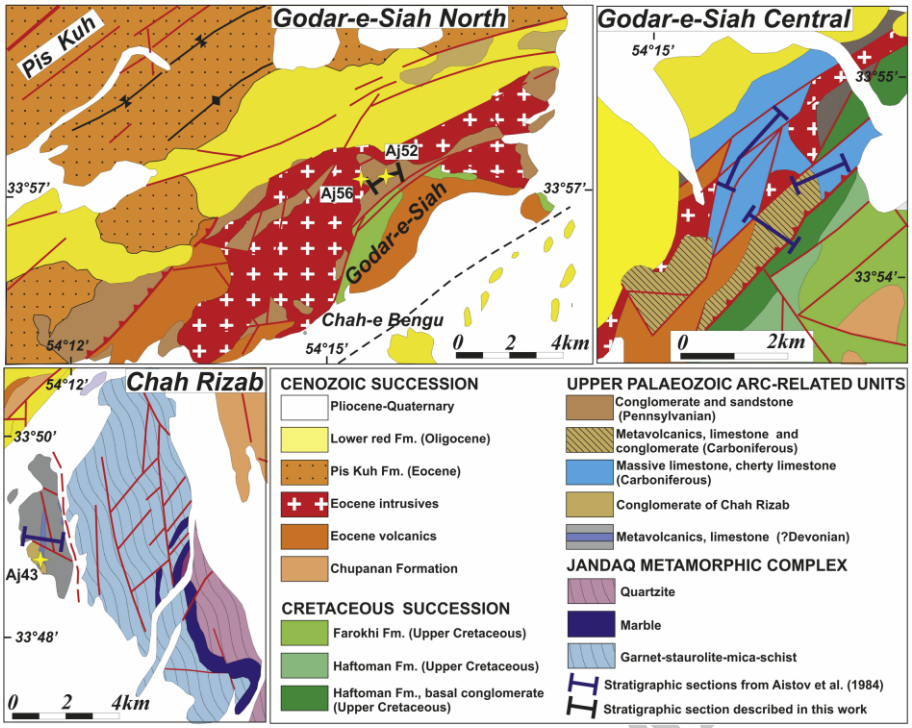

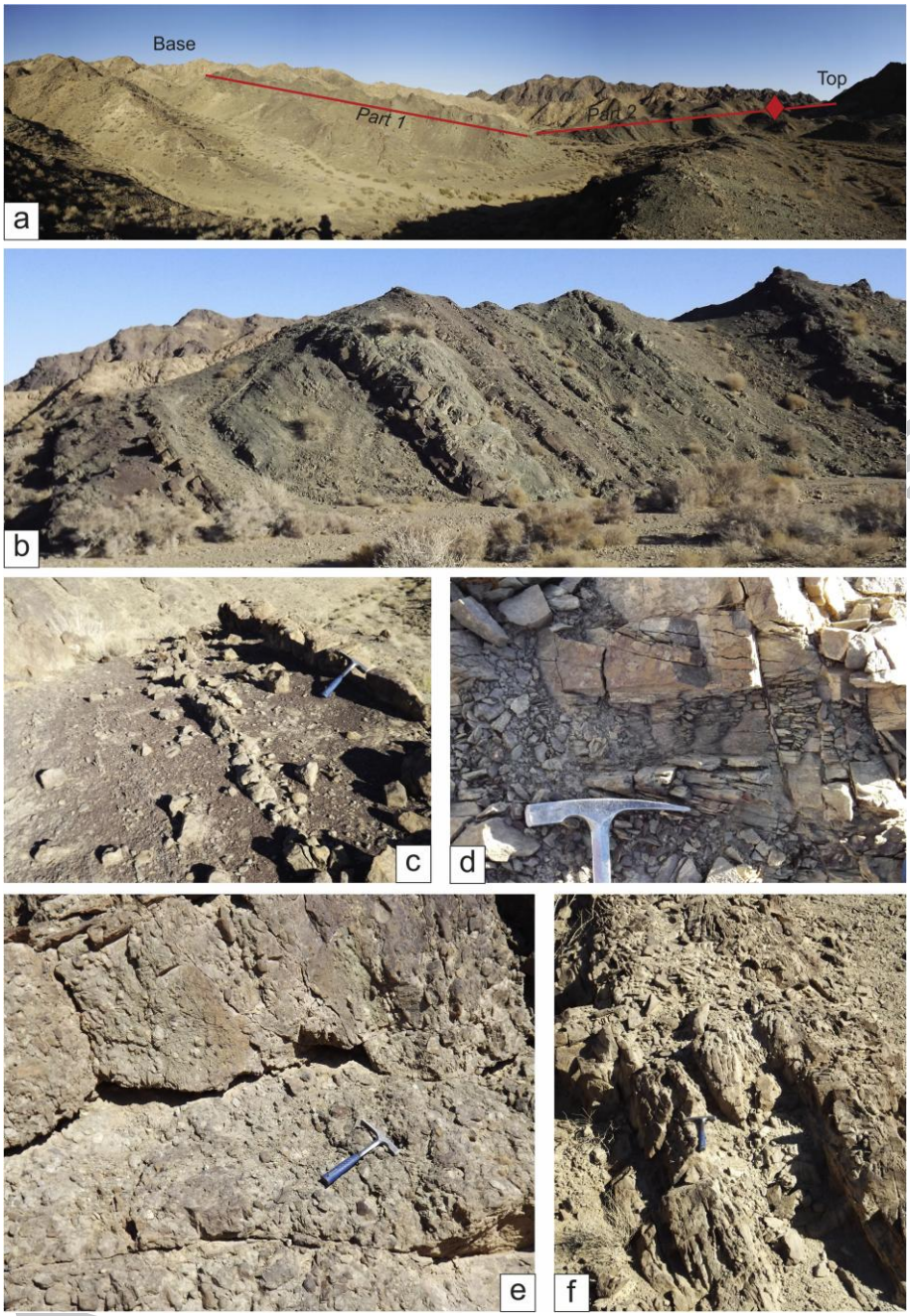

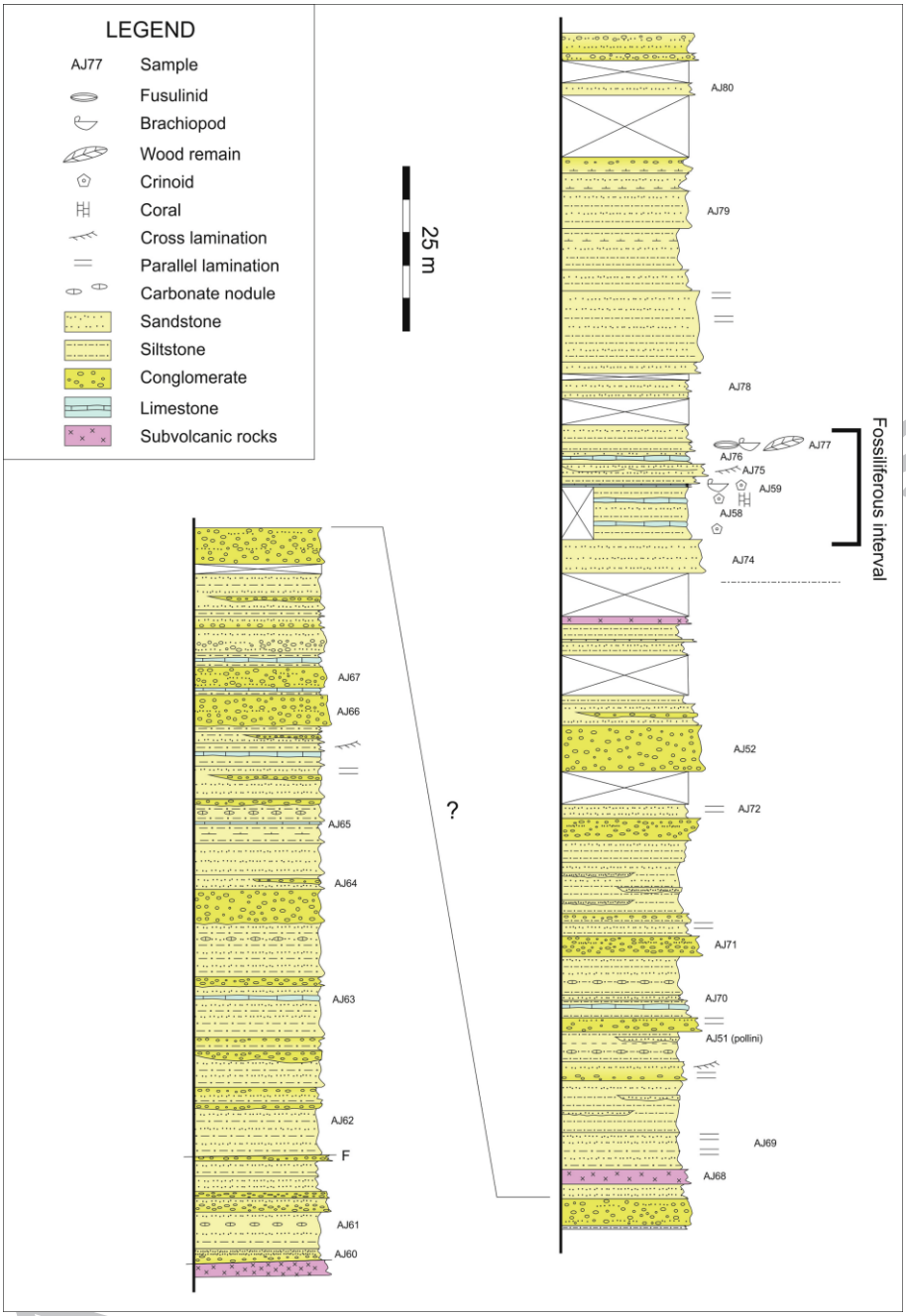

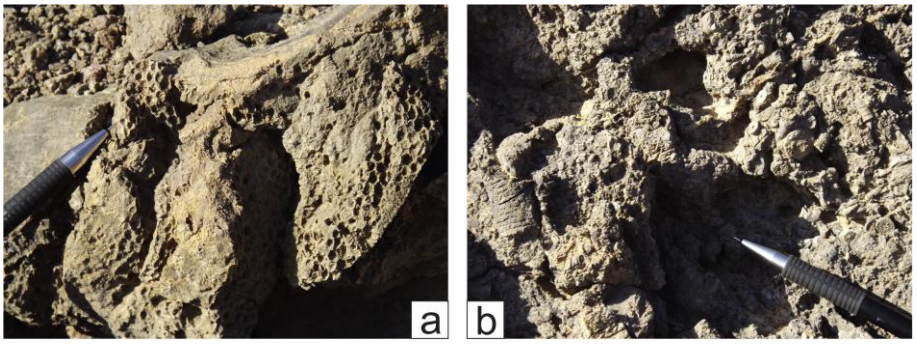

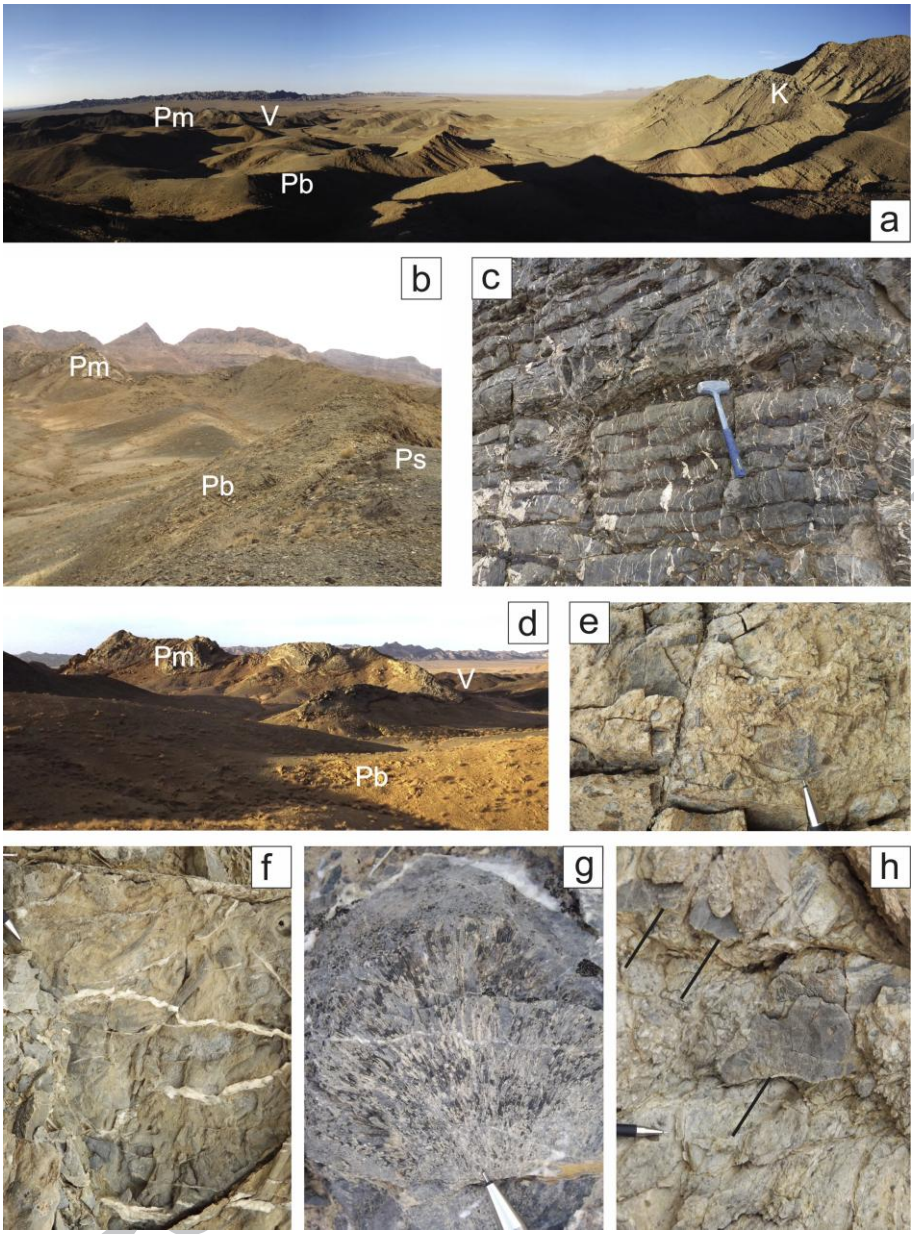

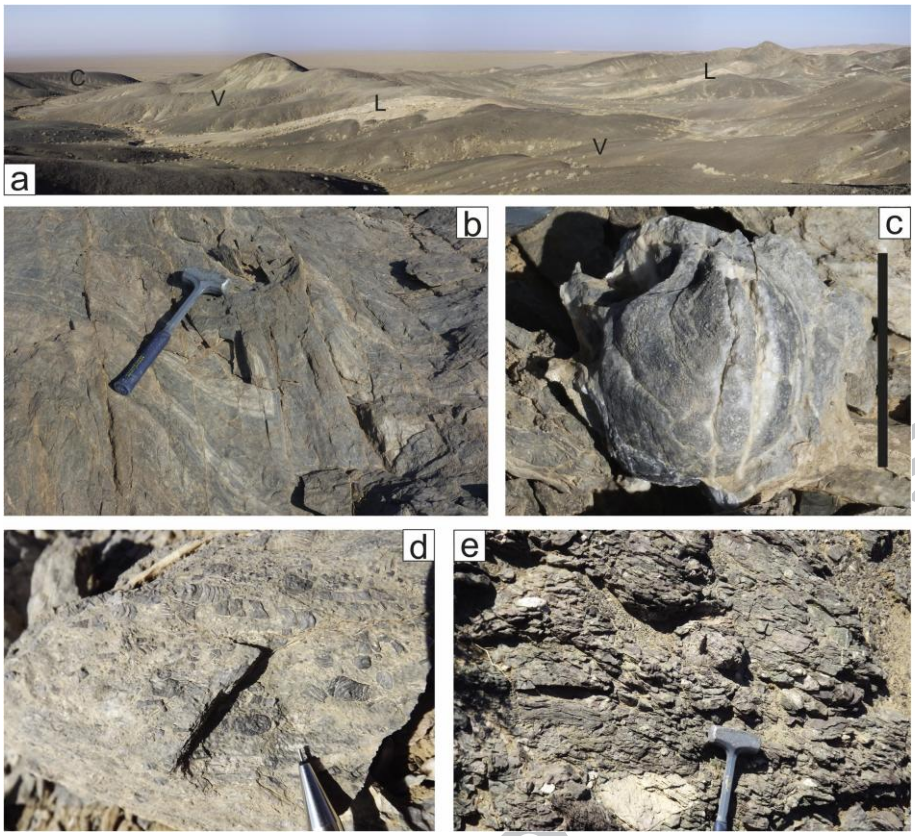

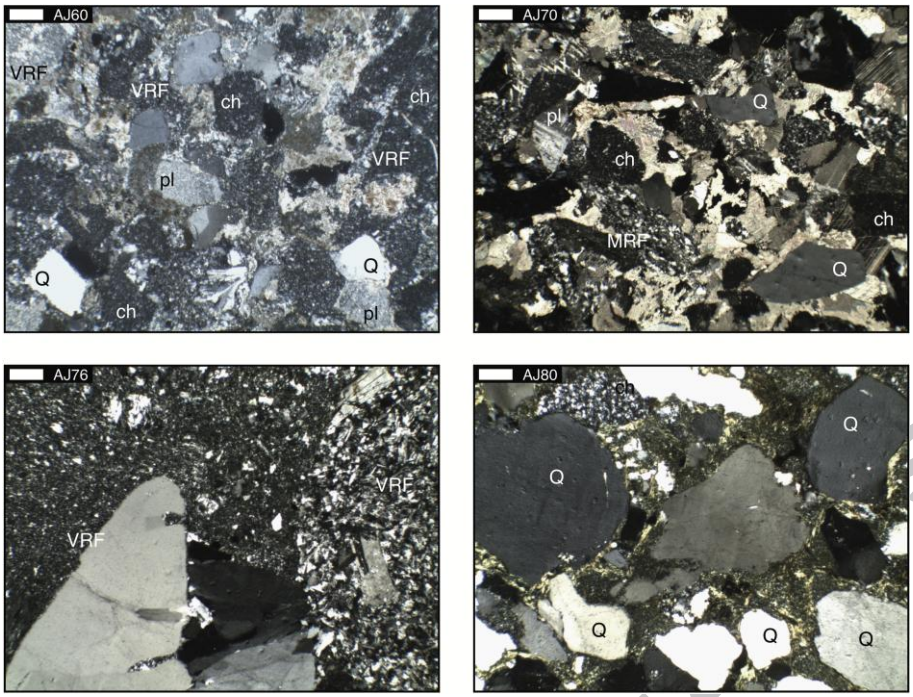

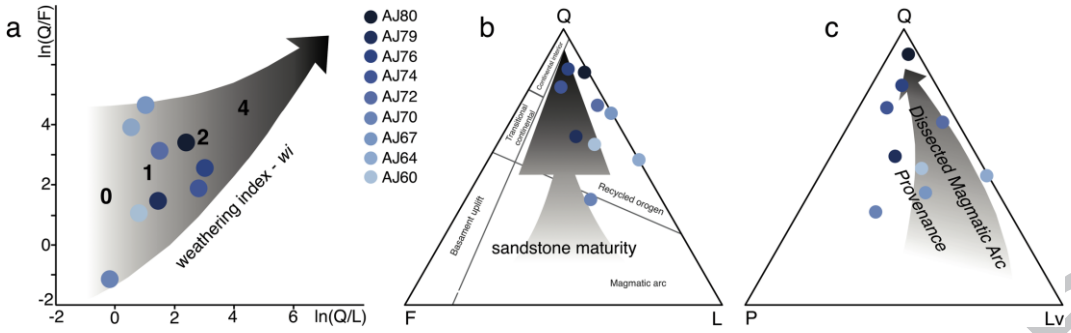

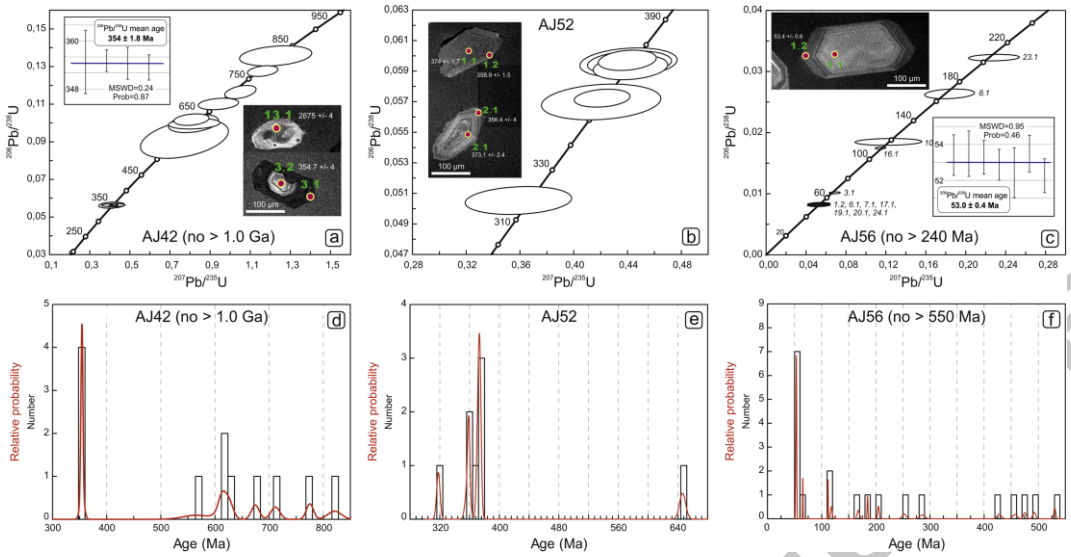

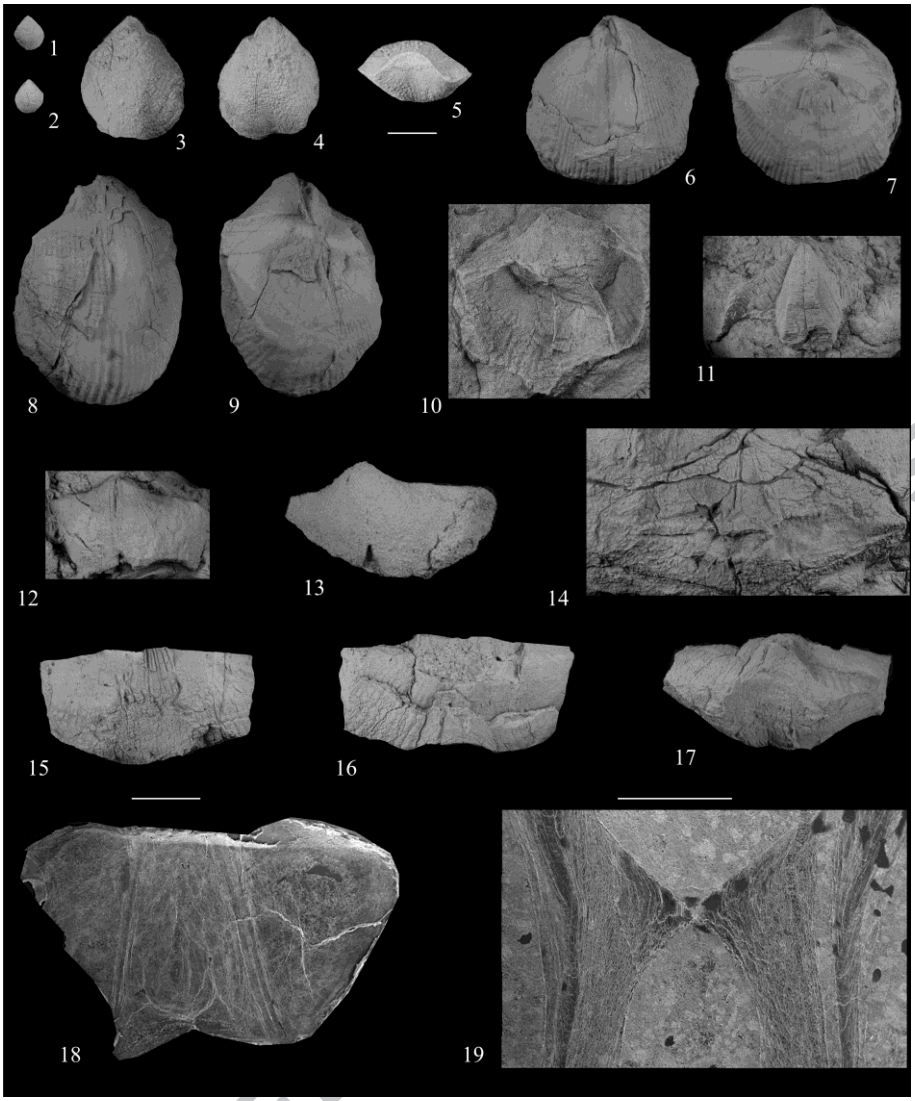

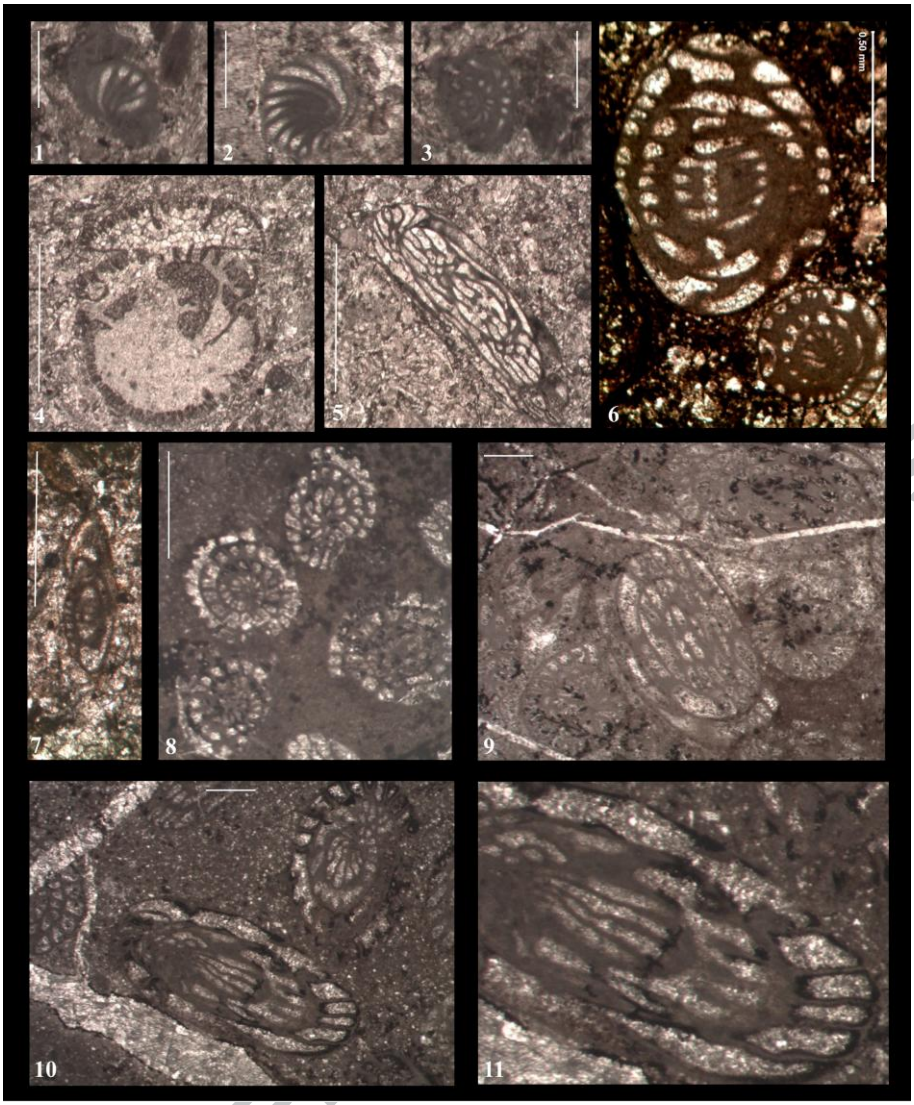

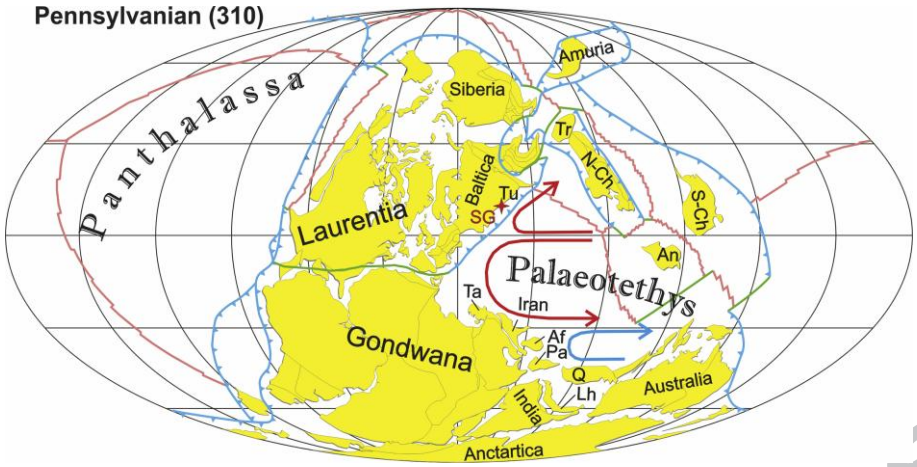

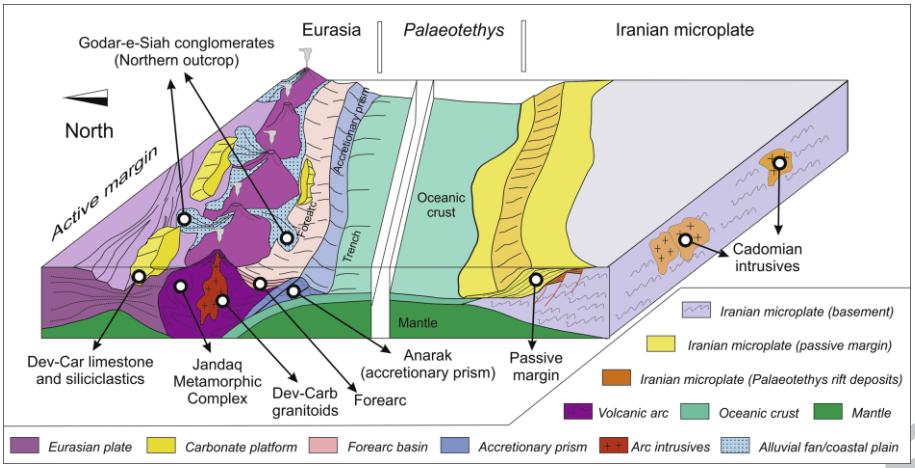

Table 1. Sample locations and analyses.

Sample	Scope	Unit	Longitude	Latitude
aj36	Brachiopods	Godar-eSiah central outcrop	54,2594	33,9092
aj37	Brachiopods	Godar-eSiah central outcrop	54,2594	33,9092
aj39	Brachiopods	Godar-eSiah central outcrop	54,2600	33,9104
aj40	Corals	Godar-eSiah central outcrop	54,2667	33,9034
aj42	Zircon U-Pb dating	Godar-eSiah northern outcrop	54,1934	33,8209
aj44	Conodonts	Chah Rizab outcrop	54,1955	33,8145
aj52	Zircon U-Pb dating	Godar-eSiah northern outcrop	54,2628	33,9495
aj56	Zircon U-Pb dating	Godar-eSiah northern outcrop	54,2616	33,9515
aj58	Brachiopods, fusulinids	Godar-eSiah northern outcrop	54,2634	33,9498
aj59	Conodonts	Godar-eSiah northern outcrop	54,2634	33,9498
aj60-80	Petrographic analysis (stratigraphic section)	Godar-eSiah northern outcrop	54,2634	33,9497
aj77	Brachiopods, fusulinids	Godar-eSiah northern outcrop	54,2634	33,9497
aj90	Corals and brachiopods	Godar-eSiah central outcrop	54,2662	33,9040

Table 2. U-Pb dating.
SHRIMP U-Pb analytical data performed on zircons separated from sample AJ42, AJ52 and AJ56.

Spot	$^{206}Pb_c$ (%)	U (ppm)	Th (ppm)	$^{232}Th/^{238}U$	$^{206}Pb^*$ (ppm)	^{204}Pb-corrected Ratios $^{207}Pb^*/^{206}Pb^*$	± 1σ (%)	$^{207}Pb^*/^{235}U$	± 1σ (%)	$^{206}Pb^*/^{238}U$	± 1σ (%)	err. corr.	Apparent Age $^{206}Pb/^{238}U$ (Ma)	± 1σ (abs.)	Apparent Age $^{207}Pb/^{206}U$ (Ma)	± 1σ (abs.)
AJ42-1.1r*	c	2852	228	0.08	106.8	0.0691	1.5	0.41	1.5	0.0433	0.4	0.235	273.5	1.0	-	-
AJ42-2.1r*	7.10	4100	388	0.10	157.7	0.0952	8.0	0.55	8.1	0.0416	1.0	0.119	262.8	2.5	-	-
AJ42-3.1r*	6.29	3257	251	0.08	152.1	0.0835	11.2	0.59	11.3	0.0509	1.2	0.110	320.2	3.9	-	-
AJ42-3.2c	0.65	211	37	0.18	10.3	0.0526	6.3	0.41	6.4	0.0566	1.2	0.180	354.7	4.0	311	72
AJ42-4.1r*	4.47	4957	387	0.08	175.2	0.0824	4.5	0.45	4.5	0.0393	0.5	0.118	248.5	1.3	-	-
AJ42-5.1r	0.63	2830	191	0.07	128.3	0.0543	1.6	0.42	1.7	0.0566	0.4	0.248	355.1	1.3	383	18
AJ42-4.2c	1.56	901	30	0.03	40.2	0.0539	5.7	0.42	5.7	0.0565	0.6	0.111	354.3	2.0	366	64
AJ42-6.1r	0.02	602	40	0.07	160.5	0.1106	2.1	4.73	2.2	0.3104	0.6	0.286	1742.7	9.6	*1810*	*19*
AJ42-7.1c	0.23	130	65	0.52	42.0	0.1262	1.4	6.53	1.8	0.3754	1.1	0.642	2054.7	20.0	*2046*	*12*
AJ42-1.2c*	2.87	75	44	0.61	13.0	0.0959	7.2	2.62	7.4	0.1978	1.9	0.255	1163.7	20.2	-	-
AJ42-8.1c	0.24	168	65	0.40	16.0	0.0620	4.2	0.94	4.4	0.1103	1.1	0.257	674.6	7.2	673	45
AJ42-9.1c	0.13	178	166	0.96	17.9	0.0653	2.8	1.05	3.0	0.1167	1.2	0.407	711.5	8.3	785	29
AJ42-8.2r	0.67	1870	313	0.17	92.3	0.0539	2.1	0.42	2.1	0.0563	0.5	0.217	353.3	1.6	368	23
AJ42-10.1c	1.57	145	160	1.14	11.6	0.0611	10.7	0.77	11.6	0.0917	4.6	0.396	565.7	24.9	642	115
AJ42-11.1c	0.00	247	109	0.45	99.3	0.1612	1.1	10.38	1.4	0.4671	0.8	0.612	2470.7	17.3	*2468*	*9*
AJ42-12.1c	0.49	194	112	0.60	17.1	0.0574	4.3	0.81	4.5	0.1020	1.2	0.275	626.4	7.3	-	-
AJ42-13.1c	0.00	407	302	0.77	174.6	0.1824	0.5	12.57	0.9	0.4998	0.8	0.824	2613.1	16.1	*2675*	*4*
AJ42-14.1c	0.88	198	70	0.37	17.1	0.0597	6.3	0.82	6.4	0.0998	1.1	0.176	613.3	6.6	-	-
AJ42-16.1c	0.12	205	41	0.21	54.4	0.1136	6.9	4.83	7.5	0.3082	3.0	0.401	1732.0	45.6	*1857*	*62*
AJ42-17.1c	0.22	95	112	1.21	11.1	0.0655	5.8	1.23	6.0	0.1358	1.6	0.269	821.0	12.4	792	60
AJ42-17.2r	0.26	244	185	0.78	26.9	0.0660	2.5	1.16	2.7	0.1278	0.9	0.337	775.3	6.6	806	26
AJ42-18.1	0.00	50	98	2.00	4.3	0.0594	5.9	0.82	6.3	0.0999	2.0	0.321	614.0	11.7	-	-

AJ52-1.1c	0.21	508	60	0.12	26.1	0.0534	1.9	0.44	2.0	0.0597	0.5	0.229	374.0	1.7	347	22
AJ52-2.1c	0.41	243	100	0.43	12.5	0.0537	3.3	0.44	3.3	0.0596	0.7	0.197	373.1	2.4	357	37
AJ52-2.2r	0.37	188	62	0.34	9.6	0.0535	4.2	0.42	4.3	0.0570	0.8	0.193	357.4	3.0	350	48
AJ52-3.1c	0.27	338	68	0.21	17.6	0.0541	2.5	0.44	2.6	0.0593	0.6	0.217	371.2	2.1	376	28
AJ52-4.1c	0.22	226	151	0.69	20.5	0.0601	2.0	0.87	2.1	0.1055	0.7	0.324	646.4	4.1	606	21
AJ52-5.1r	0.62	212	110	0.53	9.3	0.0515	4.4	0.36	4.5	0.0506	0.7	0.164	317.9	2.3	263	51
AJ52-6.1c	0.46	373	356	0.99	19.9	0.0538	2.8	0.44	2.9	0.0596	0.5	0.187	372.9	2.0	362	32
AJ52-1.2r	0.32	597	75	0.13	29.7	0.0534	2.0	0.42	2.0	0.0573	0.4	0.210	358.9	1.5	344	22
AJ56-1.1c*	0.00	14	0	0.01	0.1	0.1988	10.7	0.28	11.6	0.0101	4.5	0.390	65.1	2.9	-	-
AJ56-2.1r	0.24	280	136	0.50	19.1	0.0583	2.3	0.64	2.3	0.0794	0.6	0.243	492.6	2.7	540	25
AJ56-3.1r	0.23	879	201	0.24	7.7	0.0491	3.3	0.07	3.3	0.0101	0.6	0.194	65.1	0.4	154	38
AJ56-1.2r	1.28	435	112	0.27	3.1	0.0464	7.9	0.05	8.0	0.0083	1.1	0.132	53.4	0.6	-	-
AJ56-4.1r	0.22	863	521	0.62	21.6	0.0492	2.0	0.20	2.1	0.0291	0.4	0.201	184.8	0.8	159	24
AJ56-5.1r	0.08	995	210	0.22	73.4	0.0570	0.9	0.67	0.9	0.0858	0.3	0.335	530.5	1.6	490	10
AJ56-6.1r	1.61	339	131	0.40	2.5	0.0466	8.1	0.05	8.2	0.0083	1.2	0.145	53.5	0.6	-	-
AJ56-7.1r	1.06	583	189	0.33	4.2	0.0462	8.6	0.05	8.7	0.0083	0.9	0.103	53.3	0.5	-	-
AJ56-8.1r	0.54	221	7	0.03	5.0	0.0506	5.4	0.18	5.6	0.0263	1.2	0.222	167.6	2.0	223	63
AJ56-9.1c	0.41	139	47	0.35	8.8	0.0553	3.8	0.56	4.0	0.0735	0.9	0.228	457.1	4.0	422	43
AJ56-10.1r	1.38	194	24	0.13	3.1	0.0481	11.1	0.12	11.1	0.0185	1.2	0.109	118.1	1.4	-	-
AJ56-11.1r*	0.60	508	174	0.35	5.9	0.0517	5.5	0.10	5.6	0.0135	0.7	0.131	86.7	0.6	-	-
AJ56-12.1r*	5.23	118	12	0.10	1.0	0.1261	14.1	0.16	14.4	0.0092	2.8	0.194	58.8	1.6	-	-
AJ56-13.1r	0.23	222	107	0.50	14.6	0.0586	2.4	0.62	2.4	0.0765	0.6	0.256	475.4	2.9	551	26
AJ56-14.1ir	1.50	57	18	0.32	1.8	0.0512	12.3	0.28	12.4	0.0400	1.6	0.130	252.9	3.7	-	-
AJ56-15.1r	0.18	326	36	0.11	12.7	0.0517	2.4	0.32	2.9	0.0453	1.6	0.544	285.9	4.4	273	28
AJ56-16.1ir	0.14	1607	272	0.17	24.2	0.0476	1.9	0.11	1.9	0.0175	0.4	0.204	111.7	0.4	78	22
AJ56-17.1r	0.97	633	274	0.45	4.5	0.0474	7.6	0.05	7.6	0.0082	0.8	0.107	52.9	0.4	-	-
AJ56-18.1c	0.52	121	44	0.37	6.7	0.0563	4.4	0.53	4.5	0.0686	1.0	0.219	427.9	3.8	464	49
AJ56-19.1r	1.75	282	167	0.61	2.0	0.0469	8.7	0.05	8.8	0.0082	1.3	0.153	52.4	0.7	-	-
AJ56-20.1r	1.00	529	142	0.28	3.8	0.0462	8.5	0.05	8.6	0.0083	1.0	0.112	53.5	0.5	-	-
AJ56-21.1c	0.03	659	105	0.16	176.5	0.1120	0.6	4.81	1.0	0.3117	0.7	0.776	1748.9	11.4	*1832*	*5*
AJ56-22.1r*	0.60	356	76	0.22	12.8	0.0949	3.7	0.54	3.8	0.0416	0.7	0.181	262.7	1.8	-	-
AJ56-23.1r	0.64	361	85	0.24	10.1	0.0513	4.5	0.23	4.6	0.0323	0.7	0.148	204.7	1.4	255	52

AJ56-24.1r	0.97	575	222	0.40	4.1	0.0476	8.2	0.05	8.2	0.0081	0.9	0.110			52.3	0.5	-	-

Notes:

Errors are 1-sigma; Pb_c and Pb^* indicate the common and radiogenic portions, respectively. Common Pb corrected using measured ^{204}Pb.

Error in Standard calibration was 0.32 % (not included in above errors but required when comparing data from different mounts).

c: core; r: rim; ir: inner rim. Discarded spots: * discordant anlyses due to suspected Pb loss, high error or suspected metamictic zircon; ** high common $^{206}Pb_c$ portion.

Graphical abstract

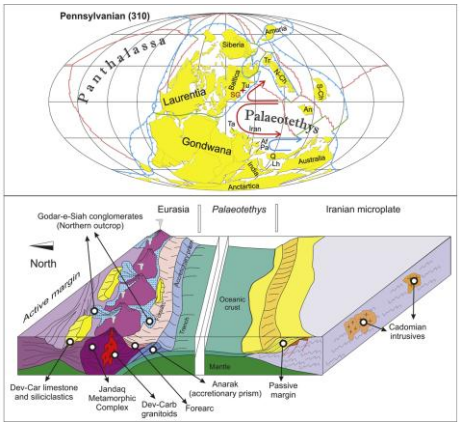

Highlights

The Godar-e-Siah Complex of Central Iran is a fragment of the Palaeotethys suture

The active margin related magmatic arc is Carboniferous based on U-Pb zircon ages

The Godar-e-Siah faunas show a N-Palaeotethyan affinity